Received: 23 May 2023 | Revised: 31 January 2024 | Accepted: 7 February 2024

DOI: 10.1111/bph.16410

RESEARCH ARTICLE

Differing contributions of the gut microbiota to the blood pressure lowering effects induced by first-line antihypertensive drugs

Cristina González-Correa[1,2] | Javier Moleón[1,2] | Sofía Miñano[1] | Iñaki Robles-Vera[3] | Marta Toral[1,2,4] | Antonio Manuel Barranco[1,2] | Natividad Martín-Morales[5] | Francisco O'Valle[2,5] | Eduardo Guerra-Hernández[6] | Manuel Sánchez[1,2] | Manuel Gómez-Guzmán[1,2] | Rosario Jiménez[1,2,4] | Miguel Romero[1,2] | Juan Duarte[1,2,4]

[1]Department of Pharmacology, School of Pharmacy and Center for Biomedical Research (CIBM), University of Granada, Granada, Spain

[2]Instituto de Investigación Biosanitaria de Granada, ibs. GRANADA, Granada, Spain

[3]Centro Nacional de Investigaciones Cardiovasculares (CNIC), Madrid, Spain

[4]Ciber de Enfermedades Cardiovasculares (CIBERCV), Madrid, Spain

[5]Department of Pathology, School of Medicine, University of Granada, Granada, Spain

[6]Department of Nutrition and Bromatology, University of Granada, Granada, Spain

Correspondence
Manuel Gómez-Guzmán, Department of Pharmacology, School of Pharmacy, University of Granada, 18071 Granada, Spain.
Email: mgguzman@ugr.es

Iñaki Robles-Vera, Centro Nacional de Investigaciones Cardiovasculares (CNIC), Madrid, Spain.
Email: roblesverai@ugr.es

Funding information
Agencia Estatal de Investigación (AEI); Ministerio de Ciencia e Innovación (MCIN), Grant/Award Number: PID2020-116347RB-

Abstract

Background and Purpose: This study analyses whether first-line antihypertensive drugs ameliorate the dysbiosis state in hypertension, and to test if this modification contributes to their blood pressure (BP) lowering properties in a genetic model of neurogenic hypertension.

Experimental Approach: Twenty-week-old male Wistar Kyoto rats (WKY) and spontaneously hypertensive rats (SHR) were untreated or treated with captopril, amlodipine or hydrochlorothiazide. A faecal microbiota transplantation (FMT) experiment was also performed by gavage of faecal content from donor SHR-treated groups to SHR recipients for 3 weeks.

Key results: Faeces from SHR showed gut dysbiosis, characterized by lower acetate- and higher lactate-producing bacteria and lower strict anaerobic bacteria. All three drugs increased the anaerobic bacteria proportion, captopril and amlodipine restored the proportion of acetate-producing bacterial populations to WKY levels, whereas hydrochlorothiazide decreased butyrate-producing bacteria. Captopril and amlodipine decreased gut pathology and permeability and attenuated sympathetic drive in the gut. Both drugs decreased neuroinflammation and oxidative stress in the hypothalamic paraventricular nuclei. Hydrochlorothiazide was unable to reduce neuroinflammation, gut sympathetic tone and gut integrity. FMT from SHR-amlodipine to SHR decreased BP, ameliorated aortic endothelium-dependent relaxation to acetylcholine,

Abbreviations: ACE, angiotensin-converting enzyme; AML, amlodipine; BP, blood pressure; F/B, Firmicutes/Bacteroidetes; FMT, faecal microbiota transplantation; HCTZ, hydrochlorothiazide; HR, heart rate; HW/TL, heart weight/tibia length; I-FABP, intestinal fatty acid-binding protein 2; KW/TL, kidney weight/tibia length; LDA, Linear Discriminant Analysis; LVW/TL, left ventricle weight/tibia length; MLN, mesenteric lymph nodes; MUC, mucin; PEG-SOD, superoxide dismutase conjugated to polyethylene glycol; PSS, physiological saline solution; PVN, paraventricular nucleus; RNP, rat neutrophil peptide; SBP, systolic blood pressure; SCFAs, short chain fatty acids; SHR, spontaneously hypertensive rat; TBST, Tris buffer saline with Tween 20; Th, T helper; Tregs, regulatory T cells; WKY, Wistar Kyoto rat; ZO-1, zonula occludens-1.

Cristina González-Correa, Javier Moleón and Sofía Miñano contributed equally as first authors.

Miguel Romero and Juan Duarte contributed equally to the supervision of the study.

I00; Junta de Andalucía, Grant/Award Numbers: CTS 164, P20_00193, A-CTS-318-UGR20

lowered NADPH oxidase activity, aortic Th17 infiltration and reduced neuroinflammation, whereas FMT from SHR-hydrochlorothiazide did not have these effects.

Conclusions and Implications: First-line antihypertensive drugs induced different modifications of gut integrity and gut dysbiosis in SHR, which result in no contribution of microbiota in the BP lowering effects of hydrochlorothiazide, whereas the vasculo-protective effect induced by amlodipine involves gut microbiota reshaping and gut-immune system communication.

KEYWORDS

amlodipine, captopril, endothelial dysfunction, gut dysbiosis, hydrochlorothiazide, hypertension, immune system

1 | INTRODUCTION

Systemic arterial hypertension is the most commonly occurring modifiable risk factor in cardiovascular disease around the world (Guzik et al., 2007; Touyz et al., 2020). The underlying cause for the rise in blood pressure (BP) and sometimes even its development can remain undetermined and undetected. New data suggests a possible role for shifts in gut bacterial populations in hypertension (Li et al., 2017; Toral et al., 2019; Yang et al., 2015). This link between BP and the composition of gut microbiota has been shown in demonstrations of dysbiosis (Yang et al., 2015), the generation of 'humanized mice' via administration of faecal microbiota from hypertensive human subjects to germ-free animals (Li et al., 2017), or the transplant from spontaneously hypertensive rat (SHR) donors into Wistar Kyoto (WKY) normotensive rats that results in a rise in sympathetic activity and BP (Toral et al., 2019). Nonetheless, how the microbiota is capable of regulating BP is not fully understood. Recent evidence has shown that neuroinflammation might be involved in this regulatory phenomenon, forming a dysfunctional gut-brain axis in high BP conditions (Robles-Vera et al., 2021; Toral et al., 2019; Xia et al., 2021). This mechanism has been further proven with the involvement of the sympathetic response in the gut, and intestinal **noradrenaline** (NA) and **tyrosine hydroxylase** concentrations (Toral et al., 2019). Interestingly, drugs such as **minocycline** (Santisteban et al., 2015; Sharma et al., 2019), **mycophenolate** (Robles-Vera et al., 2021), **spironolactone** (González-Correa et al., 2023) or exercise (Xia et al., 2021), reduce neuroinflammation, thus improving gut dysbiosis.

A bidirectional interaction between the gut microbiota and antihypertensive agents has been described. It has been recently demonstrated that the gut microbiota plays a role in the metabolism of antihypertensive drugs and thus contributes to the pathophysiology of resistant hypertension (Yang et al., 2022). There is mounting evidence from human subjects that points to first-line antihypertensive drugs acting to modulate the gut microbiota. Metagenomic analyses of faecal samples has shown links between β-blockers and **angiotensin-converting enzyme** (ACE) inhibitors and changes in the bacterial populations of the gut microbiota (Zhernakova et al., 2016). A high throughput drug screening proved that antibiotic-like effects on the gut microbiota with use of the calcium channel blockers **felodipine** and **bepridil** (Maier et al., 2018), and sulfonamide diuretics, such as **hydrochlorothiazide** (HCTZ), involves antimicrobial activity by inhibiting the bacterial **dihydrofolate reductase** enzyme (Kaur et al., 2020). Finally, antihypertensive medications may have additive effects: diuretics combined with β-blockers, ACE inhibitors or **aspirin** were associated with enriched abundance of *Roseburia*, (Forslund et al., 2021) a bacterium involved in the production of the metabolite **butyrate**, shown to lower BP in animal models (Muralitharan et al., 2020). While we still do not understand the impact of these changes on BP, evidence in SHR supports the suggestion that actions of the ACE inhibitor **captopril** (CAP) (Yang et al., 2019) and the **angiotensin II AT_1 receptor** blocker **losartan** (Robles-Vera, Toral, de la Visitación, Sánchez, Gómez-Guzmán, Muñoz, et al., 2020) may be partially dependent on the gut microbiota. However, it is unknown if the

What is already known?

- Gut microbiota is involved in the control of blood pressure (BP).
- Changes to the gut microbiota composition induced by captopril contributes to the antihypertensive effects.

What does this study add?

- Changes in gut microbiota induced by amlodipine contributed to the reduction of BP.
- Changes in microbiota did not contribute to the antihypertensive effects of hydrochlorothiazide.

What is the clinical significance?

- Gut microbiota represents a new target for amlodipine in the BP control.

antihypertensive effects of diuretics, such as HCTZ, or calcium channel blockers, such as **amlodipine** (AML), are related to changes in gut microbiota. Moreover, it is unknown how antihypertensive drugs modulate gut dysbiosis in hypertension, in addition to their antibiotic-like effects. Interestingly, captopril (Yang et al., 2019) or losartan (Robles-Vera, Toral, de la Visitación, Sánchez, Gómez-Guzmán, Muñoz, et al., 2020) decreased BP, improved gut dysbiosis, permeability and general gut pathology, and decreased neuroinflammation in the SHR, showing the key role of the renin-angiotensin system (RAS) in controlling the gut-brain axis in hypertension. By contrast, the vasorelaxant drug **hydralazine** decreased BP but was unable to improve gut dysbiosis, because of increased gut sympathetic drive (Robles-Vera, Toral, de la Visitación, Sánchez, Gómez-Guzmán, Muñoz, et al., 2020). However, whether HCTZ or AML decreases neuroinflammation in the central nuclei that play a role in autonomic control of BP, such as the hypothalamic paraventricular nucleus (PVN), known to regulate sympathetic outflow that also is involved in gut microbiota control, is not known. Hence, we studied the effects of first-line antihypertensive drugs on the bacterial composition of the gut and gut pathology and permeability. We further analysed the involvement of these changes in the BP lowering effects in a well-known model of neurogenic hypertension, presenting sympathetic activation, the SHR (Nishihara et al., 2012).

2 | METHODS

2.1 | Animals and experimental groups

All protocols involved in this study followed European Union regulations and requirements on the protection of animals used for scientific purposes, the ARRIVE guidelines (Percie du Sert et al., 2020) and the recommendations made by the *British Journal of Pharmacology* (Lilley et al., 2020) and were approved by the Ethics Committee of Laboratory Animals of the University of Granada (Spain; permit number 16/02/2022/013/A). We chose SHR as an animal model of genetic hypertension because it resembles essential hypertension in non-obese humans, and male have higher BP than female young adults (Doggrell & Brown, 1998). Twenty-weeks-old male SHR and WKY rats were obtained from Janvier Labs (Le Genest-Saint-Isle, Saint Berthevin Cedex, France) to be used in the study. Studies were performed to generate groups of equal size and sufficient statistical power. Animals were randomized to treatment groups and the experimenter was blinded to drug treatment until data analysis.

2.1.1 | Experiment 1

Rats were allotted into the subsequent groups, in individual ventilated cages: (a) untreated WKY (WKY, 1 ml of vehicle [methylcellulose 1%] day^{-1} by gavage for 5 weeks, n = 8), (b) untreated SHR (SHR, 1 ml of vehicle day^{-1}, n = 8), (c) SHR treated with captopril (SHR + CAP, 85 $mg{\cdot}kg^{-1}{\cdot}day^{-1}$ by gavage for 5 weeks, n = 6) (Santisteban et al., 2017), (d) SHR treated with AML (SHR + AML, 10 $mg{\cdot}kg^{-1}{\cdot}day^{-1}$ by gavage for 5 weeks, n = 8) (Sharifi et al., 1998), and (e) SHR treated with HCTZ (SHR + HCTZ, 90 $mg{\cdot}kg^{-1}{\cdot}day^{-1}$ by gavage for 5 weeks, n = 8) (Sano & Tarazi, 1987). Food and water intake were recorded daily, and the animals could access both ad libitum. Body weight was examined once a week. Drugs treatment was stopped 48 h before the killing of the animals for tissue collection for long-term effects assessment, avoiding the possible masking acute administration effects.

In order to analyse the effects of first-line antihypertensive drugs in control rats, we tested the effects of captopril, AML and HCTZ in normotensive WKY rats, using the same doses for 5 weeks.

2.1.2 | Experiment 2

To investigate the role of microbiota from SHR-treated groups in their antihypertensive effects, a faecal microbiota transplantation (FMT) experiment was carried out. Thus, faecal contents were collected fresh and pooled from individual SHR, SHR + AML and SHR + HCTZ rat groups at the end of the Experiment 1. Twenty-week-old recipient SHR were orally gavaged with donor faecal contents for three consecutive days, and once every 3 days for a total period of 3 weeks. Animals were randomly assigned to three different groups of eight animals each: SHR with SHR microbiota (S-S), SHR with SHR + AML microbiota (S-SAML) and SHR with SHR + HCTZ microbiota (S-SHCTZ). Rats were maintained in a specific pathogen-free environment, and were provided with water and standard laboratory diet (SAFE A04, Augy, France) ad libitum. Each rat was housed in a separate cage. Water was changed every day, and both water and food intake were recorded daily for all groups.

2.2 | Faecal microbiota transplantation (FMT)

The FMT was carried out as previously detailed by our group (Toral et al., 2019). A faecal slurry was generated from stool samples in sterile phosphate buffered saline (PBS) at a 1:20 dilution factor, the mixture was vortexed and then centrifuging at 60 *g* for 5 min to eliminate faecal debris. We collected and kept at −80°C the supernatant until used. Seven days before the transplant, we orally gavaged the recipient rats with 1-ml **ceftriaxone sodium** (400 $mg{\cdot}kg^{-1}{\cdot}day^{-1}$) for five consecutive days. Two days after finishing the treatment with ceftriaxone, we administered the animals with the donor faecal solution (1 ml) prepared as explained above.

2.3 | Blood pressure measurements

The rats were trained for 2 weeks for vehicle administration. Systolic blood pressure (SBP) and heart rate (HR) measurements were determined at basal levels before the experimental procedure. SBP and HR were obtained at room temperature by tail-cuff plethysmography as detailed in previous articles (Vera et al., 2007). In order to directly

register intra-arterial BP, once the experiment was completed, animals from Experiment 1 were surgically implanted with a polyethylene catheter with 100 U **heparin** in an isotonic, sterile NaCl solution in the left carotid artery under **isoflurane** anaesthesia. After 24 h post-surgery, intra-arterial BP measurements were recorded uninterruptedly for 60 min with a sampling frequency of 400 s^{-1} (McLab; AD Instruments, Hastings, UK). For intergroup comparisons, BP values recorded during the last 30 min were averaged. All measurements were performed in a quiet room by the same, blinded, experimenter.

2.4 | Evaluation of the contribution of sympathetic activity

To evaluate the role of sympathetic activity, we repeated Experiment 1, and intraarterial BP was recorded. Acute BP responses to intravenous injection of **hexamethonium** (30 mg·kg^{-1}), a nicotinic cholinergic antagonist that act as ganglionic blocker (Liu et al., 2022), were analysed in conscious rats. Pre-hexamethonium injection, arterial blood samples (0.2 ml) were collected through the catheter to determine NA levels. Then, the animals were completely exsanguinated under isoflurane anaesthesia, then the brain was retrieved, snap-frozen in liquid nitrogen and kept at −80°C until processed for quantitative-polymerase chain reaction (qPCR) measurements (Romero et al., 2017). In addition, coronal hypothalamic slices, including the paraventricular nucleus (PVN) were obtained using standard procedures as previously described (Dange et al., 2015).

2.5 | Tissue collection and cardiac and renal weight indices

After the experimental procedure, the rats underwent fasting overnight and then were administered 2.5-ml·kg^{-1} equitensin (500 ml contain 43% w/v chloral hydrate in 81-ml **ethanol**; 4.86-mg **nembutal**; 198-ml propylene glycol; 10.63-g $MgSO_4$; distilled water) (i.p.). This choice of equitensin, a potent anaesthetic, was made due to its appropriateness for terminal procedures where recovery is not expected, following ethical standards and study protocol requirements. Subsequently, the terminal phase was completed through blood collection from the abdominal aorta, which also effectively ensured the killing of the animals. The heart, kidney and brain tissues were also excised and processed. All tissues were preserved by snap freezing them in liquid nitrogen and then storing them at −80°C.

2.6 | Histological evaluation of gut pathologies and immunohistochemical staining in gut and brain

Tissue samples ex vivo from colon and brain were retrieved and processed for conventional morphological analysis, as previously described (Santisteban et al., 2017; Xia et al., 2021), and stained for Masson's trichrome, Movat's pentachromic and haematoxylin–eosin (H&E). A BX42 light microscope (Olympus Optical Company, Ltd., Tokyo, Japan) with a 20X objective was used to study the samples by taking 10X images with a CD70 camera (Olympus Optical Company, Ltd.) attached to the microscope. We quantified relevant parameters such as wall smooth muscle length, connective tissue area, submucosal vascular smooth muscle layer in vessels less than 70 μm; cell count (goblet cells per 100 epithelial cells), or structure depth (depth of crypts) on the images with ImageJ programme (http://imagej.nih.gov/ij/).

Immunohistochemical techniques in gut were conducted to localize of tight junction proteins including occludin, and zonula occluden protein-1 (ZO-1) in colon samples. Briefly, after deparaffinizing and rehydrating slides, they were treated in a pretreatment thermal PT module (Thermo Fisher Scientific Inc., Waltham, MA, USA) with 1 mM EDTA buffer (pH 8) for 20 min at 95°C, blocked with histoblock solution (PBS-Triton 0.01%; bovine serum albumin [BSA] 2%; horse serum 5%; goat serum 5%) for 1 h, and incubated with the primary antibodies rabbit anti-occludin (1:400; Abcam, Cambridge, USA Cat# ab216327, RRID:AB_2737295), and rabbit anti-ZO-1 (1:200; Invitrogen, Carlsbad, CA, USA Cat# 61-7300, RRID:AB_2533938), for 1 h at room temperature in the dark. All antibodies were diluted in histoblock solution. After washing with PBS, sections were incubated with the micropolymer conjugated with peroxidase and diaminobenzidine (Vitro-Master Diagnóstica, Granada, Spain) in an automated immunostainer (Autostainer480S, Thermo Fisher Scientific Inc.). Controls without primary antibody were also run in parallel.

For immunohistochemical study, cross sections of brain (4 μm) were dewaxed, hydrated and antigen unmasked with 1-mM EDTA buffer pH 8.0 (Vitro, Granada, Spain) in the PT module for 20 min at 95°C. The immunostain was carried out simultaneously in an Autostainer 480S automatic immunostainer (Thermo Fisher Scientific Inc), incubated a room temperature with rabbit primary antibody anti-Iba1 diluted 1:1000 (Invitrogen, Cat# PA5–27436, RRID:AB_2544912) for 30 min, using the technique of micropolymer (anti-mouse + anti-rabbit) conjugated with peroxidase and developed with diaminobenzidine (Master Polymer, Vitro). We used a millimetre scale in the eyepiece of a microscope (BH2, Olympus Optical Company Ltd) with a 40X objective to count the number of Iba1 positive microglial cells per mm^2. Results were expressed as numbers of positive cells per square millimetres per 0.062 (correction value for 40X magnification). A double-blind evaluation was carried out by trained researchers (F.O. & N.M.-M.). Immunohistochemistry procedures were performed in compliance with the recommendations made by the *British Journal of Pharmacology* (Alexander et al., 2018).

2.7 | Plasma determinations

Plasma was obtained from blood by centrifuging for 10 min at 2000 *g* and 4°C. The resulting plasma was aliquoted and stored at −80°C until used. **Lipopolysaccharide** (LPS) and NA concentrations in plasma and intestinal fatty acid-binding protein 2 (I-FABP) levels were

measured through commercially available kits (the Amebocyte Lysate Chromogenic Endotoxin Quantitative Kit, Lonza, Valais, Switzerland; the noradrenaline ELISA kit, IBL International, Hamburg, Germany; and the I-FABP ELISA kit, R&D Systems, Minneapolis, MN, USA), following the manufacturer's protocols.

2.8 | Vascular reactivity studies

The aorta was excised and segmented into rings (3 mm) that were mounted on organ chambers with Krebs solution (in mM: NaCl 118, **$NaHCO_3$** 25, **glucose** 11, KCl 4.75, $CaCl_2$ 2, KH_2PO_4 1.2, $MgSO_4$ 1.2) as described previously (Gómez-Guzmán et al., 2011). Vascular reactivity to acetylcholine (10^{-9} to 10^{-4} M) was studied in these segments pre-contracted with **phenylephrine** (10 μM). For an in-depth analysis of vascular relaxation capabilities, curves were performed in the presence of **N^G-nitro-L-arginine methyl ester** (L-NAME, a non-selective competitive inhibitor of **nitric oxide synthase**, 10^{-4} M), VAS2870 (non-selective inhibitor of **NADPH oxidase**, 5 μM), or with **Y27632** (**Rho kinase** inhibitor, 0.1 μM) for 30 min. In some experiments the relaxant response curves to acetylcholine were constructed after 6 h of incubation with physiological saline solution (PSS) or with **IL-17a** neutralizing antibody (nIL17, 10 $\mu g \cdot ml^{-1}$). Results are expressed as a percentage of precontraction tension levels.

2.9 | In situ detection of vascular reactive oxygen species (ROS) content

Unfixed thoracic aortic rings were cryopreserved (PBS, 0.1 $mol \cdot L^{-1}$, plus 30% **sucrose** for 1–2 h), placed in optimum cutting temperature compound medium (Tissue-Tek; Sakura Finetechnical, Tokyo, Japan), frozen (−80°C), and 5-μm cross sections were obtained in a cryostat (Microm International Model HM500 OM, Walldorf, Germany). Sections were incubated for 15 min in Hepes buffered solution, containing dihydroethidium (DHE) (10^{-6} M), counterstained with the nuclear stain **DAPI** (3×10^{-7} M) and in the following 24 h examined on a fluorescence microscope (Leica DM IRB, Wetzlar, Germany). Sections were photographed and fluorescence was quantified using the ImageJ programme. All parameters (pinhole, contrast, gain and offset) were held constant for all sections from the same experiment. ROS production was estimated from the ratio of ethidium/DAPI fluorescence (Zarzuelo et al., 2011). dihydroethidium (DHE) fluorescence was also analysed in aortic sections from the SHR group incubated for 30 min, at 37°C, in the presence of superoxide dismutase conjugated to polyethylene glycol (PEG-SOD, 25 $U \cdot ml^{-1}$) before dihydroethidium (DHE).

2.10 | NADPH oxidase activity

A scintillation counter (Lumat LB 9507, Berthold, Germany) was used to measure NADPH oxidase activity in aorta, using a lucigenin-enhanced chemiluminescence method as previously described in detail by our group (Zarzuelo et al., 2011), by incubating tissue samples at 37°C for 30 min in an HEPES buffer solution (in mM): $CaCl_2$ 1.2, glucose 5.5, HEPES 20, KCl 4.6, KH_2PO_4 0.4, $MgSO_4$ 1, NaCl 119, $NaHCO_3$ 1. The chemiluminescent signal was achieved by adding 100-μM **NADPH** as a substrate for the reaction and 5-μM lucigenin to be oxidised proportionally to the amount of ROS generated, emitting light as a signal.

Alternatively, enzyme activity from PVN samples was measured by fluorescence derived from dihydroethidium (DHE) oxidation products incubated with tissue homogenates, as done previously (Toral et al., 2019). We incubated the samples at 37°C for 30 min in PBS with 10-μM dihydroethidium (DHE) and 1.25-$\mu g \cdot ml^{-1}$ DNA, 100-μM diethylenetriamine pentaacetate (DTPA) and 50-μM NADPH in the absence or in the presence of the NADPH oxidase inhibitor apocynin (50 μM). The fluorescent signal was studied, exciting at 490 nm and detecting the emission at 590 nm in a Fluostart fluorescence spectrometer (BMG Labtechnologies, Offenburg, Germany). NADPH oxidase activity was defined as the difference between values obtained in the absence and those obtained in the presence of apocynin.

2.11 | Reactive oxygen species (ROS) concentrations in the PVN

ROS concentration in the PVN was studied using the fluorescent probe 5-(and-6-)chloromethyl-2′-7′-dichlorodihydrofluorescein diacetate (CM-H2DCFDA, 5 μM) from tissue homogenates in a non-denaturing lysis buffer (50-mM Tris–HCl, 10 $\mu g \cdot ml^{-1}$ aprotinin, 0.1-mM EDTA, 0.1-mM EGTA, 10-$\mu g \cdot ml^{-1}$ leupeptin, 1-mM PMSF) for 30 min at 37°C. Fluorescence was measured in the Fluostart fluorescence spectrometer as described previously (Toral et al., 2019).

2.12 | Flow cytometry

Mesenteric lymph nodes (MLN) and aortae were adequately homogenized for cell collection. Blood was treated with Gey's solution for red cell lysis. Then, all samples were filtered through a 40-μM cell strainer. 1×10^6 cells per sample were counted and incubated at 37°C with 50-$ng \cdot ml^{-1}$ **PMA**, 1-$\mu g \cdot ml^{-1}$ ionomycin and a protein transport inhibitor (BD GolgiPlugTM) for a total of 4 h 30 min. Non-specific staining was prevented. blocking with anti-CD32 (clone D34-485, BD Biosciences), while staining for live/dead (LIVE/DEAD® Fixable Aqua Dead cell Sain Kit, Molecular Probes, Oregon, USA). Cells were then stained in sequential incubations for extracellular and intracellular markers. The samples were also permeabilized and fixed. The list of antibodies and their targets used can be found in Table S1. Flow cytometry was performed on a FACS ARIA III flow cytometer (BD Biosciences) and the final analysis was carried out using FlowJo software (Tree Star, Ashland, OR, USA) as described previously (González-Correa et al., 2023). Gate strategy for flow cytometry is showed in Figure S1.

2.13 | Gene and protein expression analysis

To determine gene expression levels in colon and PVN, we performed quantitative PCRs as previously done (González-Correa et al., 2023). RNA was obtained by tissue homogenization with TRI Reagent®. The probes utilized can be found in Table S2. All qPCR reactions were carried out in a Techne Techgene thermocycler (Techne, Cambridge, UK). The mRNA relative expression was determined using the ΔΔCt method.

We used western blots to look at the levels of ZO-1 and occludin in colonic homogenates. These samples were electrophoresed with sodium dodecyl sulphate-polyacrilamide (20 μg of protein per lane). The proteins were then transferred to polyvinylidene difluoride membranes. Then, membranes were blocked with 5% bovine serum albulin (BSA) in Tris Buffer Saline with Tween 20 (TBST) solution (0.5 M Tris pH 7.5; 1.5 M NaCl; 0.1% Tween 20) for 1 h. After incubating the membranes with the appropriate primary antibodies, ZO-1 and occludin were detected: rabbit polyclonal anti-occludin (1:1000, Abcam, Cambridge, USA Cat# ab216327, RRID:AB_2737295) and rabbit polyclonal anti-tight junction protein ZO-1 (1:1000; Invitrogen, Carlsbad, CA Cat# 61-7300, RRID:AB_2533938). All were incubated at 4°C overnight at 1/1000 dilution. The membranes were then exposed with Santa Cruz Biotechnology's secondary peroxidase-conjugated goat anti-rabbit (1/10000). All antibodies were diluted in TBST with 3% of BSA. An ECL system (Amersham Pharmacia Biotech, Amersham, UK) was used to detect antibody binding, and ImageJ software was used to perform densiometric analysis. Smooth muscle ß-actin was again found in the samples. For each control or experimental sample, the relative abundance of the protein of interest was normalized to the mean of the controls to minimize variations. All quantifications were carried out by a blind analyser. Western blot procedures were performed in compliance with the recommendations made by the *British Journal of Pharmacology* (Alexander et al., 2018).

2.14 | DNA extraction, 16S rRNA gene amplification, bioinformatics

A detailed version of the protocol can be found in our previous publications (Toral et al., 2019) DNA from faecal samples was extracted using G-spin columns at the end of the experiment (INTRON Biotechnology). Amplification of the V4-V5 regions was carried out for the 16S rRNA. Amplicon libraries were obtained from Bioanalyzer 2100 (Agilent). Sequencing was performed using the Illumina MiSeq instrument with 2 × 300 paired-end read sequencing at the Unidad de Genómica (Parque Científico de Madrid, Spain). USEARCH6.1 was used for operational taxonomic unit (OTU) generation. The Taxonomy Database (National Center for Biotechnology Information) was utilized for classification and nomenclature. Bacteria were classified according to their short chain fatty acid (SCFA) end-products, as established previously (Xia et al., 2021).

2.15 | Reagents

The chemicals and other reagents were purchased from Merk (Barcelona, Spain) unless otherwise specified.

2.16 | Statistical analysis

Data and statistical analysis comply with the recommendations of the *British Journal of Pharmacology* on experimental design and analysis in Pharmacology (Curtis et al., 2022). Initial group size (n = 8) was selected for the Experiments 1 and 2, and n = 6 for drugs-treated control WKY experiment, based on our previous experience, considering the possible loss of rats due to the application of the criteria of humane endpoints; if physical signs other than drugs treatment were observed, loss of consumption data, failure during mounting the aorta in the organ bath, insufficient amount of tissue for quantitative PCRs, during the surgery for the in vivo, or outlier values (determined by the extreme studentized deviate method [ROUT test] with significance level of $Q = 1$). These conditions were the only exclusion criteria employed and account for differences in group sizes. A smaller group size of n = 5 was considered for the ex vivo determinations due to lower intrinsic variability, resulting in fewer expected outliers and less expected data loss due to simpler procedures. In all experiments, the size group was described in the section on animals and experimental groups, and it refers to biological samples rather than technical replicates.

The reads per operational taxonomic unit (OTU) were standardized to the total number of reads per sample. We used Phyloseq tools to calculate the Chao and Shannon indexes. In the analysis, we included only the data from taxa prevalent in over 20% of the samples and over four reads per sample. We show the Linear Discriminant Analysis (LDA) only for scores over 3.5, at genus level. The analysis was performed using the Microbiome Analyst for the Linear Discriminant Analysis effect size (LEfSe) (Chong et al., 2020), considering the enrichment significant at $P < 0.05$. Results are expressed as means ± SEM. Features with significant differential abundant were identified through the non-parametric factorial Kruskal-Wallis sum-rank test. The analysis was accompanied by LDA to determine the effect size of each differentially abundant feature. Beta diversity of the microbiota was determined via comparisons of bacterial composition of thousands of taxa between two samples. All samples are compared to the other samples resulting in a distance or dissimilarity matrix, that was analysed through the Bray–Curtis distance and represented by Principal Coordinate Analysis (PCoA).

Data analysis was performed using Prism v8 (GraphPad Sofware Inc., USA). Tail cuff SBP, HR and the results for the vascular reactivity tests were analyses by two-way repeated-measures ANOVA with the Bonferroni post hoc test. Alternatively, other data were tested for normal distribution through the Shapiro–Wilk normality test and compared by one-way ANOVA and Tukey post hoc test if the data presented a normal distribution or Mann–Whitney *U* test or Kruskal-

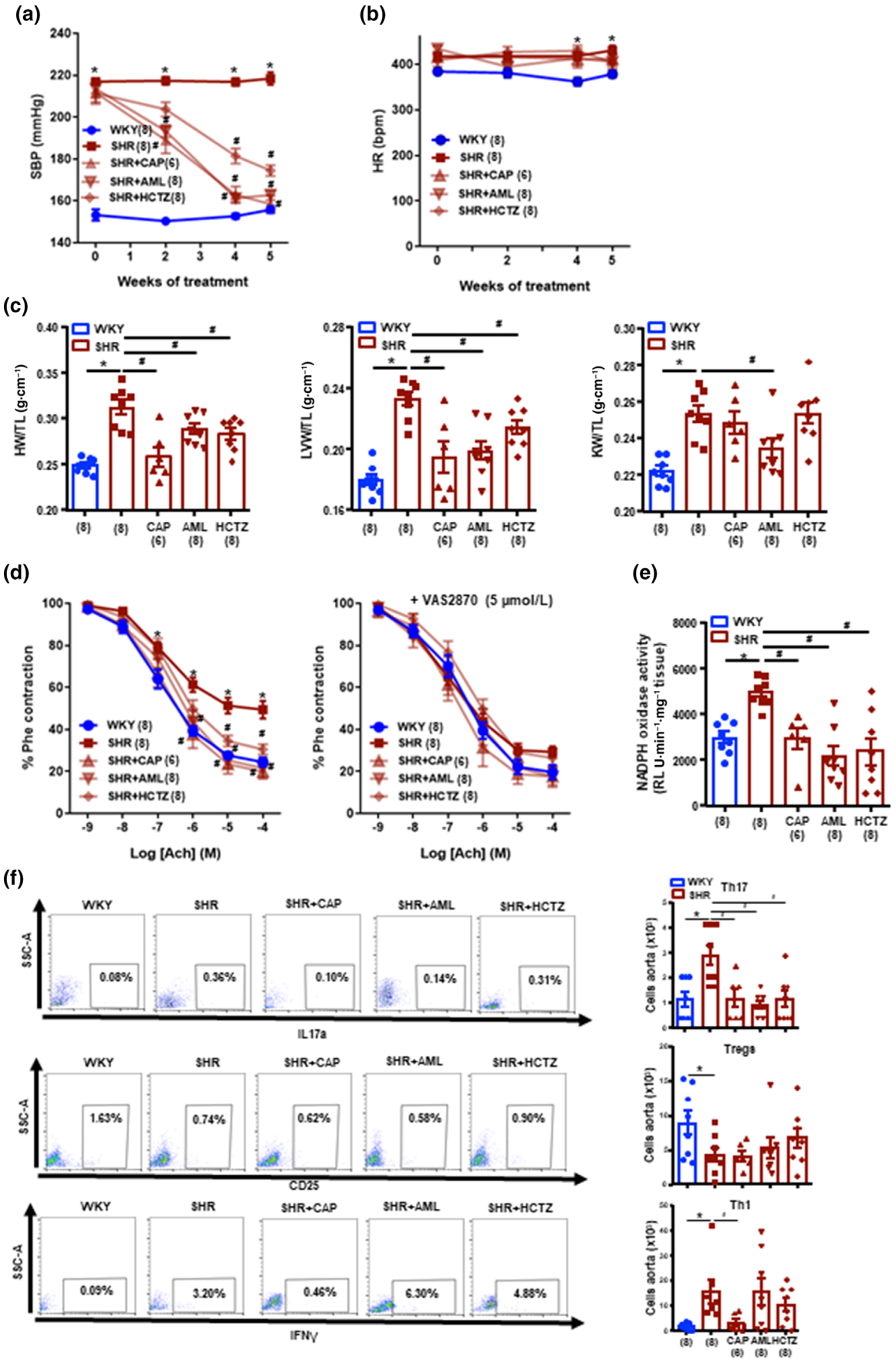

FIGURE 1 Legend on next page.

Wallis with Dunn's multiple comparison test if the distribution was abnormal. Post-hoc tests were run only if F achieved P<0.05 and there was no significant variance inhomogeneity. $P < 0.05$ was considered statistically significant.

2.17 | Nomenclature of targets and ligands

Key protein targets and ligands in this article are hyperlinked to corresponding entries in http://www.guidetopharmacology.org and are permanently archived in the Concise Guide to PHARMACOLOGY 2023/24 (Alexander, Christopoulos, Davenport, Kelly, Mathie, Peters, Veale, Armstrong, Faccenda, Harding, Davies, et al., 2023; Alexander, Fabbro, Kelly, Mathie, Peters, Veale, Armstrong, Faccenda, Harding, Davies, Annett, et al., 2023; Alexander, Fabbro, Kelly, Mathie, Peters, Veale, Armstrong, Faccenda, Harding, Davies, Beuve, et al., 2023; Alexander, Kelly, Mathie, Peters, Veale, Armstrong, Buneman, Faccenda, Harding, Spedding, Cidlowski, et al., 2023).

3 | RESULTS

3.1 | First-line antihypertensive drugs decrease BP and organ target damage and ameliorate aortic endothelial dysfunction in SHR

As expected, in comparison to their healthy counterparts, the SHR experienced a rise in the SBP and HR (Figure 1a,b). The captopril, AML or HCTZ treatments induced a progressive decrease in SBP down by ~59, 51 and 37 mmHg, respectively. Additionally, high heart weight/tibia length (HW/TL), left ventricle weight/tibia length (LVW/TL) and kidney weight/tibia length (KW/TL) ratios were detected in SHR compared with those in WKY. The three drugs improved the cardiac hypertrophy parameters, whereas only AML reduced renal hypertrophy (Figure 1c). In WKY, captopril and AML treatments slightly reduced SBP by ~13, and 8 mmHg, respectively, with HCTZ being without effect (Figure S2a). HR was similar among all experimental groups of WKY treatments (Figure S2b). In addition, aortae from SHR showed reduced endothelium-dependent vasodilation to acetylcholine in comparison to WKY (Figure 1d), and this was improved by all three drugs. The vasodilatory capabilities in all samples were completely abolished by coincubation with L-NAME, which proves the involvement of nitric oxide in the observed vasorelaxant effects (data not shown). In relaxation curves that used VAS2870, the vasodilation of SHR aortic rings reached WKY levels, pointing to a role for NADPH oxidase in SHR endothelial dysfunction (Figure 1d). This was also corroborated by the study of NADPH activity, which was increased (~1.7-fold) in SHR in comparison to WKY. All treatments were able to normalize enzyme activity values to healthy control levels (Figure 1e). Red fluorescence was measured in sections of aorta incubated with dihydroethidium (DHE) to characterize and localize ROS levels within the vascular wall. When compared to control mice, SHR rings showed significantly increased staining (~5-fold), which was significantly reduced by all antihypertensive drugs. PEG-SOD abolished increased red fluorescence in SHR, indicating its O_2^- specificity (Figure S3).

Evidence suggests that vascular T cell infiltration regulates ROS production and endothelial function in SHR (Guzik et al., 2007; Robles-Vera et al., 2021). High levels of T helper (Th)17 and Th1 cell and reduced levels of regulatory T cell (Tregs) infiltration were detected in aorta from SHR, as compared to WKY (Figure 1f). Captopril normalized Th17 and Th1 infiltration in SHR, whereas AML and HCTZ only reduced Th17 cell infiltration in the aorta.

3.2 | First-line antihypertensive drug treatment induced changes in gut microbiota in SHR

There is a proven link between microbiota and the SHR phenotype (Toral et al., 2019; Yang et al., 2015), which prompted us to examine the effects of these drugs on gut microbiota composition. Shannon and Simpson, ecological parameters of diversity and Chao and abundance-based coverage estimator, that study richness, can be used to measure alpha diversity, as well as Chao and abundance-based coverage stimator, that study richness, can all be used to measure alpha diversity. No significant changes were detected among all experimental groups in these parameters (Figure 2a). The axonometric two-dimensional Principal Coordinate Analysis (PCoA) at genus level showed no significant differences among all experimental groups (Figure 2b). HCTZ altered the intestinal microbiome populations in SHR but this was not statistically significant (Figure 2b). At phylum level, we observed minor changes in phyla proportion induced by these drugs, except HCTZ (Table S3 and Figure 2c). HCTZ reduced bacteria belonging to Firmicutes and increased Bacteroidetes; and AML reduced the relative abundance of Tenericutes. The Firmicutes/Bacteroidetes (F/B) ratio is commonly used as a marker of gut dysbiosis (Yang et al., 2015), and it is usually higher in SHR than WKY; nevertheless, in our experiment it was unaltered in SHR, being reduced by HCTZ treatment (Figure 2d). Furthermore, the populations of strict anaerobic and aerobic bacteria were reduced and

FIGURE 1 Captopril (CAP), amlodipine (AML) and hydrochlorothiazide (HCTZ) reduce blood pressure, target organ damage, endothelial dysfunction and aortic T cells infiltration in spontaneously hypertensive rats (SHR). Time course of systolic blood pressure (SBP) (a) and heart rate (HR) (b) measured by tail-cuff plethysmography. (c) Ratio heart weight/tibia length (HW/TL), left ventricle weight/tibia length (LVW/TL) and kidney weight/tibia length (KW/TL). (d) Endothelium-dependent relaxation induced by acetylcholine (Ach) in aortas precontracted by phenylephrine (phe) in the absence or in the presence of the NADPH oxidase inhibitor VAS2870. (e) NADPH oxidase activity measured by chemiluminescence to lucigenin. (f) Th17, Tregs, and Th1 infiltration measured by flow cytometry in aorta from all experimental groups. Values are expressed as mean ± SEM. The number of animals analysed is shown in parenthesis. * indicates $P < 0.05$ compared with Wistar Kyoto rats (WKY). # indicates $P < 0.05$ compared with untreated SHR group.

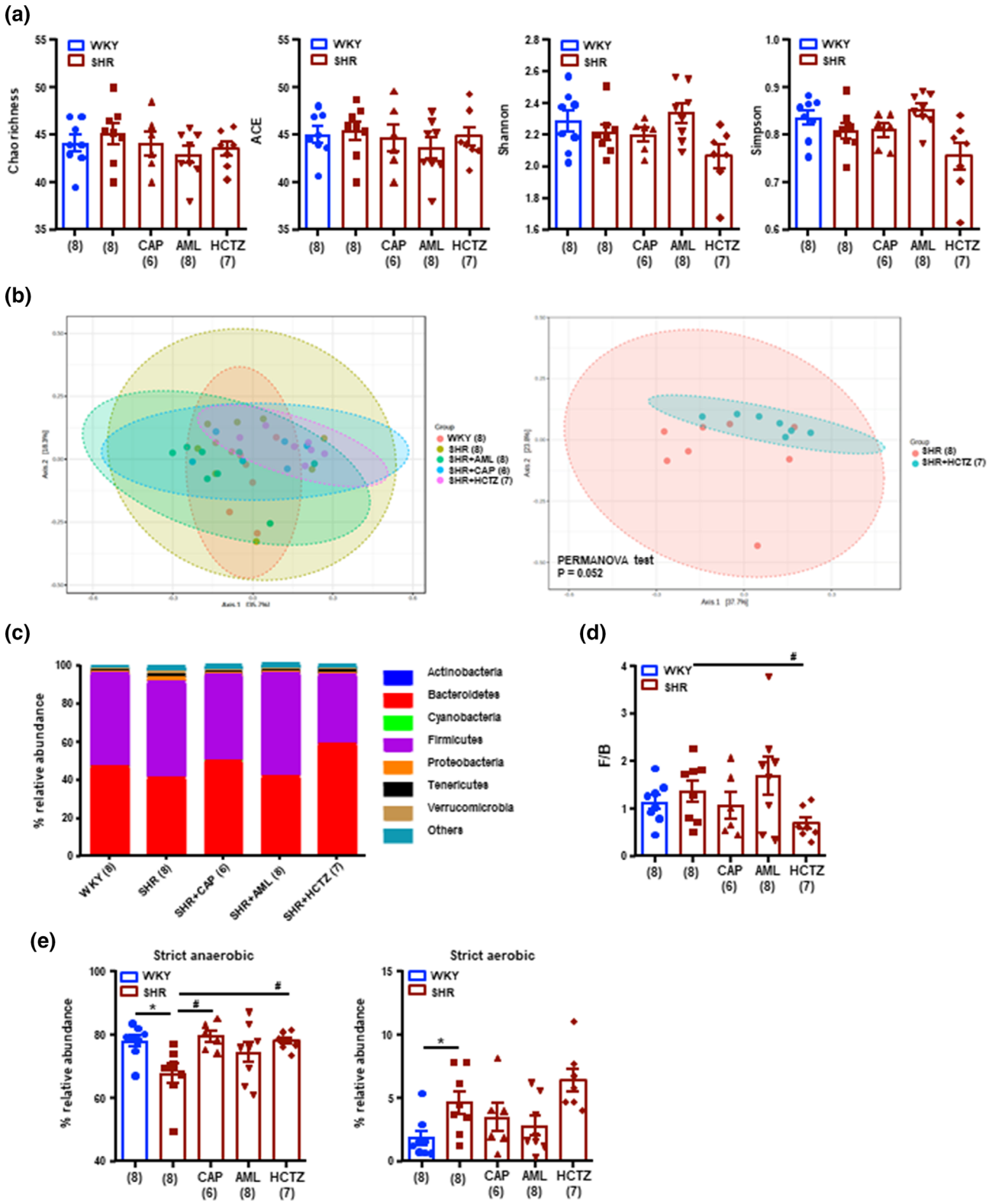

FIGURE 2 Captopril (CAP), amlodipine (AML) and hydrochlorothiazide (HCTZ) reshape the remodelling of gut microbiota in spontaneously hypertensive rats (SHR). The microbial DNA from faecal samples was analysed by 16S rRNA gene sequencing. (a) Ecological parameters of richness, such as Chao, and abundance-based coverage estimator (ACE), and diversity, such as Shannon and Simpson. (b) Principal coordinate analysis (PCoA) in the gut microbiota from all experimental groups. (c) Phylum breakdown of the seven most abundant bacterial communities in the faecal samples was obtained from all experimental groups. (d) Firmicutes/Bacteroidetes ratio (F/B ratio) was calculated as a biomarker of gut dysbiosis. (e) Relative proportion of strict anaerobic and aerobic bacteria from all experimental groups. Values are expressed as mean ± SEM. The number of animals analysed is shown in parenthesis. * indicates $P < 0.05$ compared with Wistar Kyoto rats (WKY). # Indicates $P < 0.05$ compared with untreated SHR group.

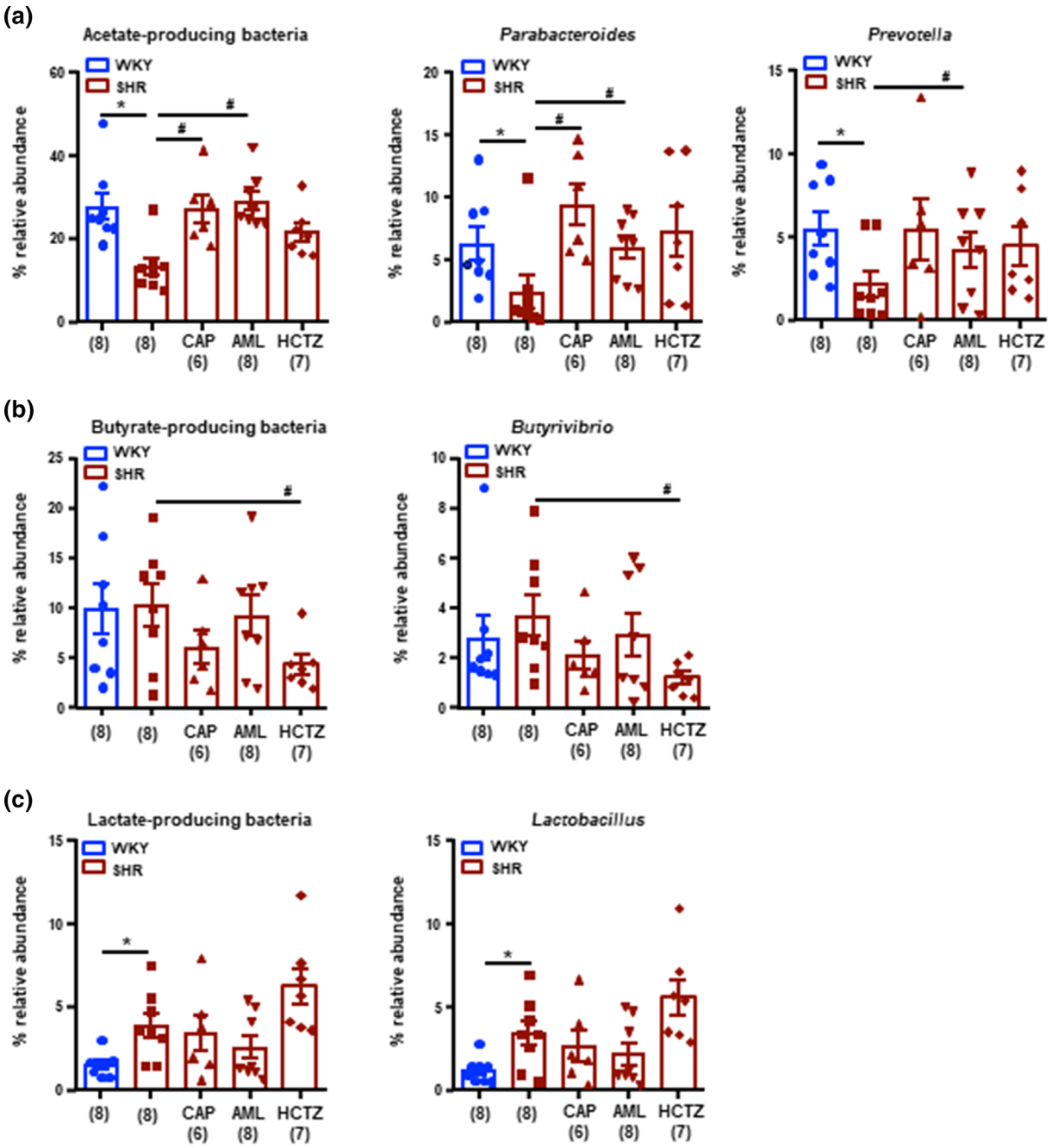

FIGURE 3 Captopril (CAP), amlodipine (AML) and hydrochlorothiazide (HCTZ) reshape the Short Chain Fatty Acid (SCFA)-producing bacteria in spontaneously hypertensive rats (SHR). Relative proportion of (a) total acetate- (b) total butyrate- and (c) total lactate-producing bacteria expressed as relative abundance of total bacteria, and main SCFA-producing genera. The microbial DNA from faecal samples was analysed by 16S rRNA gene sequencing. Values are expressed as mean ± SEM. The number of animals analysed is shown in parenthesis. * indicates $P < 0.05$ compared with Wistar Kyoto rats (WKY). # indicates $P < 0.05$ compared with untreated SHR group.

increased, respectively, in SHR in comparison to WKY (Figure 2e). Captopril and HCTZ increased the relative abundance of strict anaerobic bacteria, but not significantly modified strict aerobic population.

In WKY rats, captopril and HCTZ treatments decreased richness parameters, captopril decreased Shannon diversity, and AML had no effect on ecological parameters (Figure S4a). The axonometric two-dimensional Principal Coordinate Analysis (PCoA) at the genus level revealed statistically significant differences between all treated groups and the untreated-WKY group (Figure S4b). Both captopril and HCTZ increased Bacteroidetes and reduced the Firmicutes phylum (Figure S4c), while HCTZ increased Verrucomicrobia. Captopril and HCTZ both reduced the F/B ratio (Figure S4d). Captopril increased the populations of strict anaerobic bacteria while having no effect on the strict aerobic population (Figure S4e). In WKY, AML treatment had no effect on the relative proportion of phyla or the strict aerobic and anaerobic bacteria.

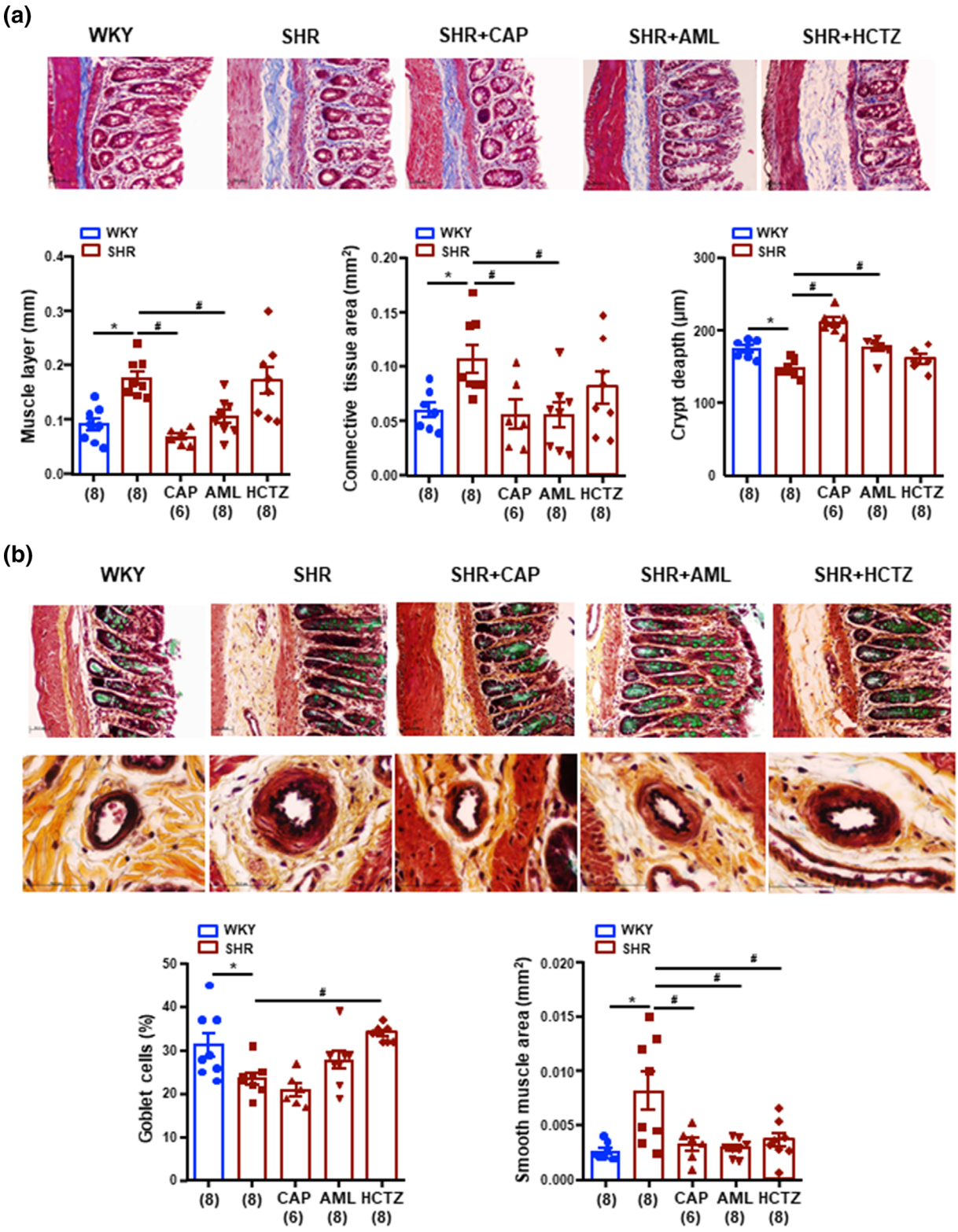

FIGURE 4 Effects of captopril (CAP), amlodipine (AML) and hydrochlorothiazide (HCTZ) on the gut pathological alterations in the colon in spontaneously hypertensive rats (SHR). (a) Representative micrographs of Masson-trichrome staining and quantitative analysis of muscle layer length, connective tissue area and crypt depth in the colon from all experimental groups. (b) Representative micrographs of Movat's pentachromic (MP) staining (upper) and representative micrographs of MP staining of the submucosal vascular smooth muscle layer (bottom) and quantitative analysis of number of goblet cells per 100 epithelial cells and the area of the submucosal vascular smooth muscle layer in vessels less than 70 µm in the colon from all experimental groups. Bar scale: 50 µm. Values are expressed as mean ± SEM. The number of animals analysed is shown in parenthesis. * indicates $P < 0.05$ compared with Wistar Kyoto rats (WKY). # indicates $P < 0.05$ compared with untreated SHR group.

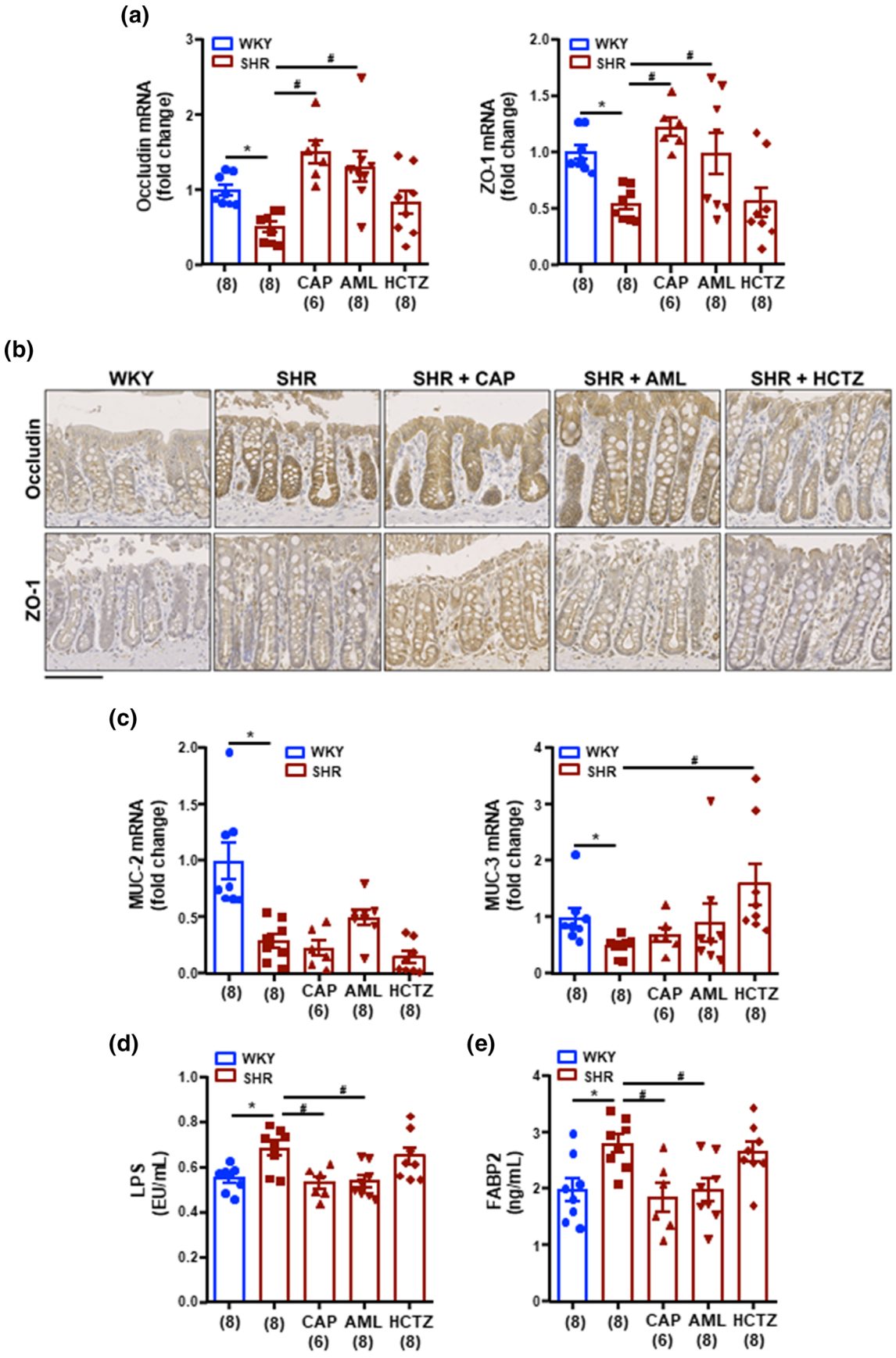

FIGURE 5 Legend on next page.

The shifts in gut microbiota in SHR are also marked by changes in the populations of SCFAs-producing bacteria (González-Correa et al., 2023; Robles-Vera et al., 2021; Robles-Vera, Toral, de la Visitación, Sánchez, Gómez-Guzmán, Muñoz, et al., 2020; Toral et al., 2019; Xia et al., 2021; Yang et al., 2015). We were able to observe a reduction in acetate-producing bacteria (Figure 3a), no detectable changes in butyrate-producing bacteria (Figure 3b) and an increase in **lactate**-producing bacteria (Figure 3c) between SHR and WKY. Interestingly, captopril and AML normalized the relative populations of acetate-producing bacteria, mainly *Parabacteroides* and *Prevotella*, whereas HCTZ significantly reduced the proportion of butyrate-producing bacteria, especially *Butyrivibrio*. No significant changes in the proportion of lactate-producing bacteria were induced by the three drug treatments. When the effects of these drugs on SCFA-producing bacteria in WKY rats were studied, captopril increased total acetate-producing bacteria, primarily by increasing *Bacteroides* and *Blautia* (Figure S5a), while decreasing butyrate-producing bacteria, primarily by decreasing the abundance of *Coprococcus* (Figure S5b). The HCTZ treatment had no effect on total acetate- and butyrate-producing bacteria, but it increased *Blautia* and decreased *Coprococcus*. Any of these drug treatments changed the relative proportion of lactate-producing bacteria in WKY rats, as it did in SHR (Figure S5c).

3.3 | First-line antihypertensive drug treatment differently affects gut pathology, inflammation, permeability, α-defensins production, and changes MLNs T cells in SHR

An increase in gut pathology and permeability and a decrease in tight junction protein expression in gut epithelial cells have been associated with the development of hypertension (González-Correa et al., 2023; Santisteban et al., 2015). SHR showed colonic thickening of the muscular layer, a rise in the connective tissue area, and a reduction in villi length in comparison to those in WKY (Figure 4a). In addition to this, a decreased percentage of goblet cells and a rise in thickness of the adventitia and connective tissue surrounding arterioles were detected in the colon of the SHR in comparison to WKY (Figure 4b). Both captopril and AML treatments decreased the connective tissue and muscular layer thickness and favoured the increase in villi length in SHR colon, with no effects in goblet cell proportion. By contrast, HCTZ was unable to improve pathological features in colon from SHR, except normalizing goblet cell content. Remarkably, the higher cross-sectional area of colonic arterioles detected in SHR in comparison to WKY were decreased by all three drugs. Then, we studied the expression of colonic proinflammatory cytokines through qPCR. The increased mRNA levels of interleukin **IL-1ß**, and tumour necrosis factor-alpha (TNF-α) in SHR compared to WKY were normalized by captopril and AML, HCTZ being without effect (Figure S6).

In addition to this, we then focused on the effects of these drugs on colonic gut integrity through the mRNA levels of tight junction proteins, zonula occludens-1 (ZO-1) and occludin, and mucins (MUC). Low levels of expression for occludin and ZO-1 were found in colon from SHR in comparison with WKY (Figure 5a). Captopril and AML treatment increased occludin and ZO-1 colonic levels, which suggests an increased barrier function. Peripheral membrane localization of both tight junction proteins was detected in immunohistochemical images from all experimental groups (Figure 5b). Additionally, high gut permeability in fully hypertensive SHR was associated with low numbers of goblet cells (Santisteban et al., 2017). Goblet cells excrete mucins that protect the gut from pathogen infiltration and regulate the gut immune response as part of a physiological barrier (Mowat & Agace, 2014). In correlation with lower goblet cells, MUC-2 and MUC-3 transcripts were down-regulated too in SHR, and MUC-3 mRNA levels were restored only by HCTZ treatment (Figure 5c). Moreover, plasma LPS levels were increased in SHR in comparison with WKY and endotoxemia was normalized by captopril and AML, but not by chronic HCTZ (Figure 5d). Our results showed increased intestinal permeability in SHR. This facilitates the migration of bacteria-derived molecules of interest (e.g., LPS) to the blood stream, and drugs able to restore gut integrity, such as captopril and AML, reduced plasma LPS levels. I-FABP2 is a broadly recognized gut permeability marker (Stevens et al., 2018), and higher circulating I-FABP levels were also detected in animals and human with hypertension (González-Correa et al., 2023; Kim et al., 2018; Stevens et al., 2018). We also found higher plasma I-FABP in the SHR group than in the WKY animals. Again, captopril and AML, but not HCTZ reduced I-FABP plasma levels (Figure 5e).

The cells that form the gut epithelium are able to synthesize defensins, peptides that possess antibiotic activity against microorganisms (Bevins, 2005), to balance the composition of the local microbiota (Hashimoto et al., 2012). In our results, SHR displays a decrease in colonic α-defensin rat neutrophil peptide (RNP)1–2 expression levels, and increased levels for RNP3 and RNP4 compared with the WKY group. Chronic captopril and AML, but not HCTZ treatment restored RPN3 and RPN4 levels to those of the WKY group (Figure S7a). By contrast, no changes were observed among all

FIGURE 5 Effects of captopril (CAP), amlodipine (AML) and hydrochlorothiazide (HCTZ) on gut integrity and permeability in spontaneously hypertensive rats (SHR). (A) mRNA levels of occludin, and zonula occludens-1 (ZO-1) in the colon in all experimental groups. (b) Representative immunohistochemistry images showing occludin- and ZO-1-positive cells in the colon from all experimental groups (scale, 100 μm). (c) mRNA levels of mucin (MUC)-2, and MUC-3 in the colon in all experimental groups. (d) Levels of plasma endotoxin (endotoxin units per millilitre [EU·ml^{-1}]). (e) Measurement of intestinal FABP levels in the plasma. Values are expressed as mean ± SEM. The number of animals analysed is shown in parenthesis. * indicates $P < 0.05$ compared with Wistar Kyoto rats (WKY). # indicates $P < 0.05$ compared with untreated SHR group.

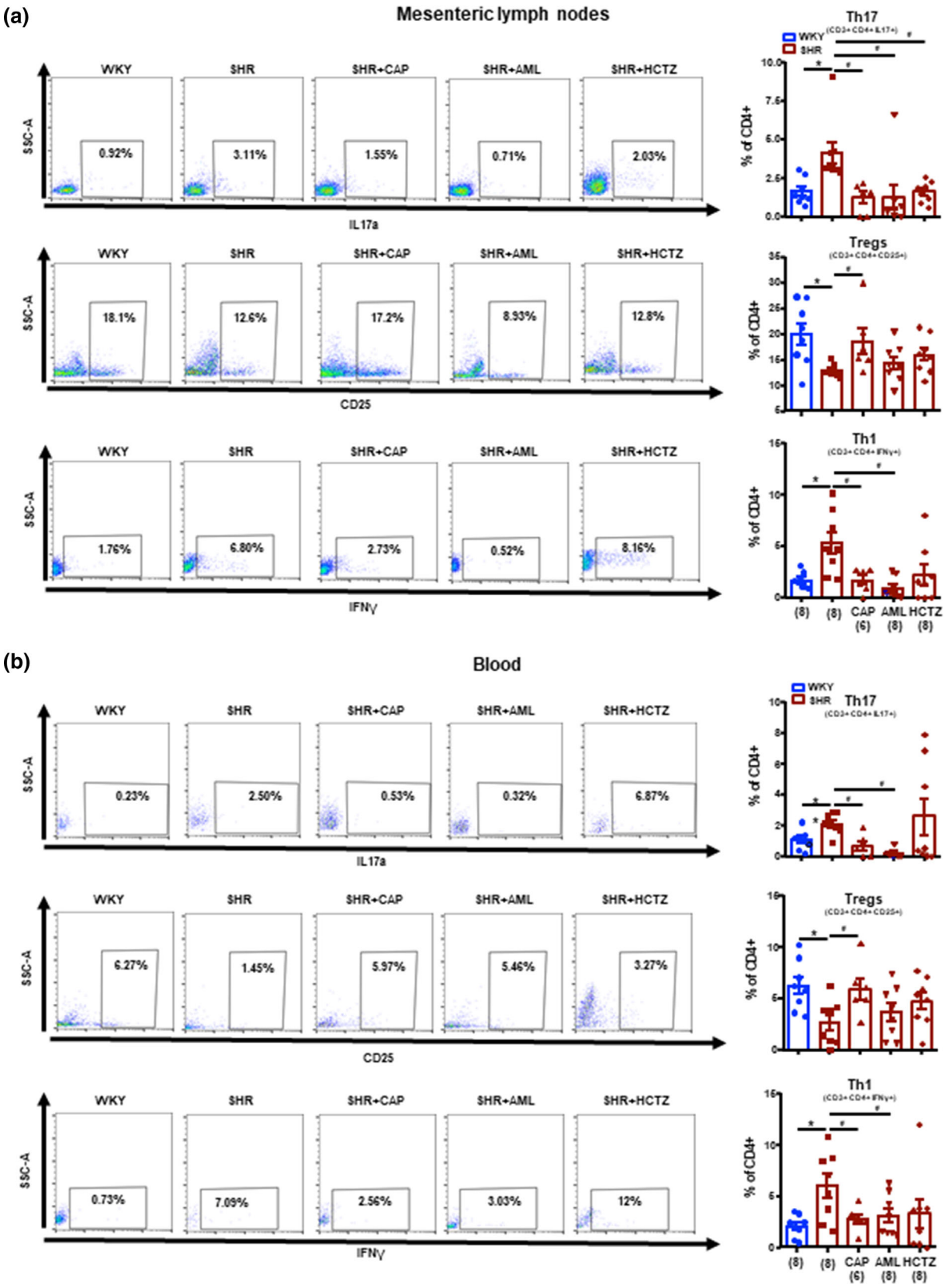

FIGURE 6 Captopril (CAP), amlodipine (AML) and hydrochlorothiazide (HCTZ) improve T cell profile at mesenteric lymph nodes (MLNs) and in blood in spontaneously hypertensive rats (SHR). T helper (Th)-17 (CD3+ CD4+ IL17a+), regulatory T cells (Treg; CD3+ CD4+ CD25+) and Th1 (CD3+ CD4+ IFNγ+) measured by flow cytometry in MLNs (a) and blood (b) from all experimental groups. Values are expressed as mean ± SEM. The number of animals analysed is shown in parenthesis. * indicates $P < 0.05$ compared with Wistar Kyoto rats (WKY). # indicates $P < 0.05$ compared with untreated SHR group.

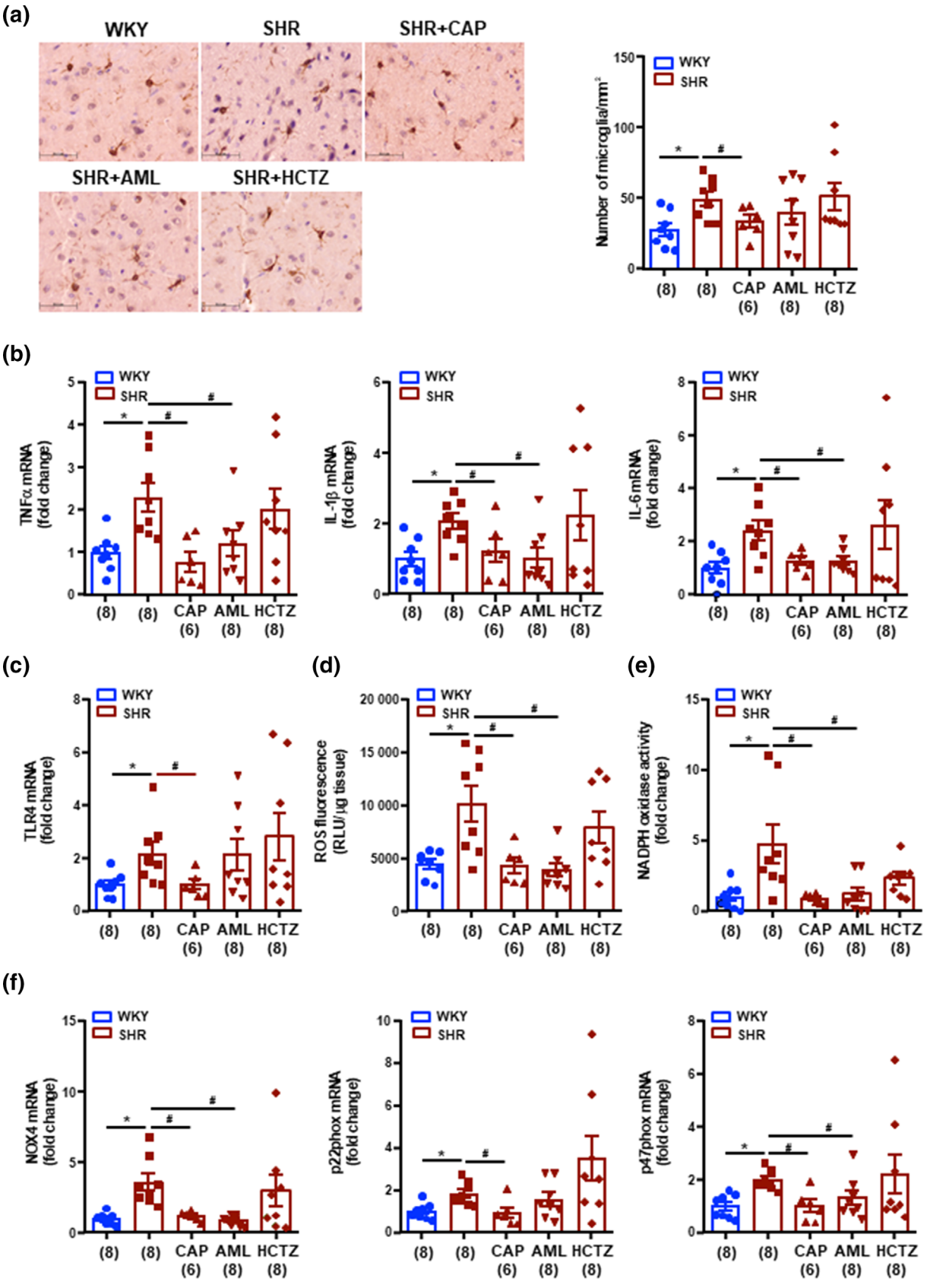

FIGURE 7 Legend on next page.

experimental groups on the mRNA levels of ß-defensins (**DefB-2**, DefB-3 and DefB-4) (Figure S7b).

It has been previously described that under altered gut mucosal integrity conditions, such as in hypertension, bacteria can move into the bloodstream through the intestinal wall, activating in their path macrophages and dendritic cells that then migrate to local lymph nodes (Niess et al., 2005). These **CX3CR1**+ cells are able to prime naïve **CD4**+ T cells into proliferation by processing and presenting bacterial antigens. In fact, in our experiment we found that Th17 and Th1 relative populations were increased in MLNs from SHR in comparison to WKY, whereas the Treg population was reduced in SHR (Figure 6a). Captopril treatment normalized Th17, Tregs and Th1 proportion in MLNs from SHR, AML reduced Th17 and Th1, and HCTZ reduced Th17 content. We observed parallelisms in the results from blood, except for HCTZ which was unable to induce any change (Figure 6b).

3.4 | First-line antihypertensive drug treatment differently protected against neuroinflammation, and gut sympathetic tone in the SHR

Hypertension has been associated with increased activated microglia, oxidative stress and neuroinflammation in autonomic brain regions (Sharma et al., 2019). In fact, in brain PVN, a key autonomic brain region in the regulation of BP, we found that the total number of microglial cells was increased in SHR as compared with WKY rats (Figure 7a) and captopril treatment normalized this parameter. Microglia activation by agents such as IFNγ and LPS induced a proinflammatory phenotype. Our group discovered that the relative expression of pro-inflammatory cytokines such as TNF-α, IL-1ß and **IL-6** were higher in SHR than in WKY (Figure 7b), and were reduced by chronic captopril and AML treatment, whereas HCTZ was without effect. **Toll like receptor TLR4** activation in the brainstem plays a role in neuroinflammation and the enhanced sympathetic outflow (Dange et al., 2015). TLR4 expression in PVN from SHR was increased in comparison to the WKY group and was reduced only by captopril treatment (Figure 7c). NADPH oxidase-derived high oxidative stress in the PVN is responsible for the increase in central sympathetic outflow (Gao et al., 2005). In PVN from SHR we showed increased ROS production (Figure 7d), NADPH oxidase activity (Figure 7e), mRNA levels of NADPH oxidase subunits, NOX4, p22phox and p47phox (Figure 7f) as compared with WKY group. Both captopril and AML, but not HCTZ reduced all these parameters.

In order to study the effects of these drugs on sympathetic outflow, we assessed the BP drop induced by the ganglionic blocker hexamethonium, and the plasma NA concentration. Basal SBP measured by intra-arterial cannula at the end of the experiment showed similar qualitative results to that registered by tail-cuff plethysmography (Figure 8a). The percentage reduction of SBP induced by hexamethonium was higher in the SHR group than WKY group. Chronic captopril and AML, but not HCTZ inhibited the drop in SBP after hexamethonium, as compared to the SHR group (Figure 8b). In addition, compared with the WKY rats, the plasma NA levels were increased in SHR, and were only reduced by captopril and AML treatment (Figure 8c), displaying a decreased sympathetic activity. A high sympathetic activity to the gut can cause alterations in gut junction proteins in SHR (Santisteban et al., 2017). We found increased concentrations of tyrosine hydroxylase (TH), an enzyme involved in the synthesis of NA, (Figure 8d) and NA levels (Figure 8e) in the colon from SHR as compared to the WKY group, which were reduced by captopril and AML but not by HCTZ treatment. These results link reduced intestinal sympathetic tone with gut pathology, integrity and permeability improvement.

3.5 | Different protective effects of faecal microbiota transplantation (FMT) from SHR-treated with antihypertensive drugs on BP and endothelial dysfunction in SHR

Previous studies in SHR demonstrated that BP lowering effects of the ACE inhibitor captopril (Yang et al., 2019) and angiotensin II type 1 receptor blockers losartan (Robles-Vera, Toral, de la Visitación, Sánchez, Gómez-Guzmán, Muñoz, et al., 2020) were partially dependent on the gut microbiota. To investigate whether shifts in populations of the intestinal microbiome induced by chronic AML and HCTZ treatments play a role in the known antihypertensive effects, we carried out an FMT from SHR treated with AML or HCTZ to untreated SHR (S-SAML and S-SHCTZ groups, respectively). For comparisons, a parallel FMT from untreated SHR to untreated SHR (S-S group) was conducted. Ceftriaxone treatment reduced SBP by ∼8 mmHg in all SHR, suggesting the regulatory capabilities of microbiota in BP control. FMT increased SBP in all experimental groups (Figure 9a). However, after 3 weeks of FMT, we found a significant decrease of ∼15 mmHg in SBP in S-SAML compared to S-S rats, whereas no changes in SBP were found between S-SHCTZ and S-S groups (Figure 9a,b). Moreover, an amelioration of the endothelium-dependent relaxation to

FIGURE 7 Effects of captopril (CAP), amlodipine (AML) and hydrochlorothiazide (HCTZ) on microglia, neuroinflammation, and ROS production in the paraventricular nucleus (PVN) of the hypothalamus in spontaneously hypertensive rats (SHR). (a) The upper pictures show the number of microglia with anti-Iba1 antibody indicative of microglia. (b) mRNA levels of pro-inflammatory cytokines, tumour necrosis factor α (TNFα), interleukin IL-1β and IL-6 and toll like receptor TLR-4 (c) in homogenates from brain PVN. (d) 5-(and-6-)chloromethyl-2′-7′-dichlorodihydrofluorescein diacetate (CM-H2DCFDA)-detected intracellular ROS and NADPH oxidase activity (e) measured by dihydroethidium (DHE) fluorescence in the microplate reader in homogenates from brain PVN. (f) mRNA levels of NADPH oxidase subunits NOX4, p22phox and p47phox in PVN. Values are expressed as mean ± SEM. The number of animals analysed is shown in parenthesis. * indicates $P < 0.05$ compared with Wistar Kyoto rats (WKY). # Indicates $P < 0.05$ compared with untreated SHR group.

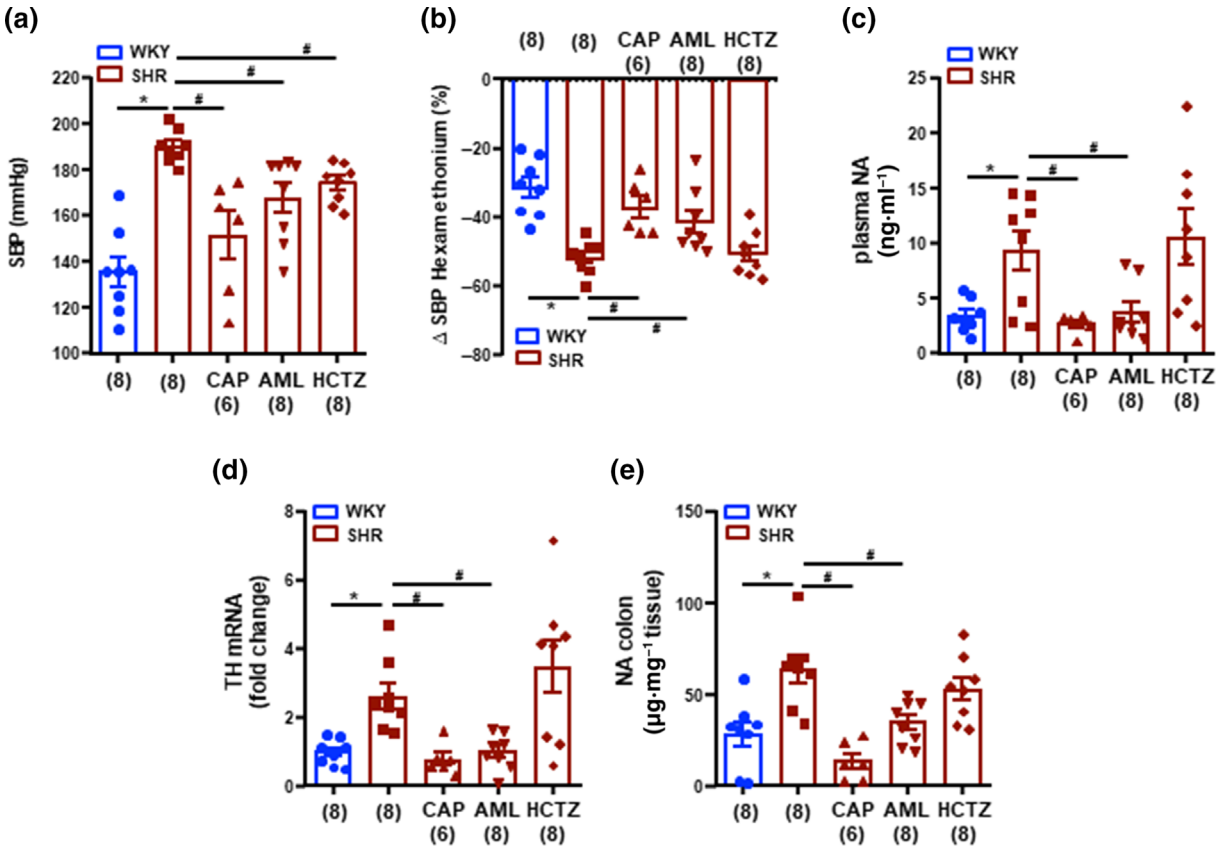

FIGURE 8 Effects of captopril (CAP), amlodipine (AML) and hydrochlorothiazide (HCTZ) on sympathetic tone. (a) Basal systolic blood pressure (SBP) measured by carotid intraarterial recording. (b) Decrease induced by acute intravenous administration of hexamethonium (30 mg kg^{-1}) on SBP in conscious rats. (C) Plasma noradrenaline (NA) content, (d) colonic tyrosine hydroxylase (TH) expression and (e) colonic NA concentration found in all experimental groups. Values are expressed as mean ± SEM. The number of animals analysed is shown in parenthesis. * indicates $P < 0.05$ compared with Wistar Kyoto rats (WKY). # indicates $P < 0.05$ compared with untreated SHR group.

acetylcholine (Figure 9c) and a lower NADPH oxidase activity (Figure 9d) and in situ ROS accumulation (Figure S8) were also induced by faecal transplant from SHR treated with AML, but not with HCTZ. In addition, NADPH oxidase inhibition with VAS2870 or Rho kinase inhibition with Y27632 improved the relaxant responses to acetylcholine in S-S and S-HCTZ groups (Figure 9c), but not in S-SAML, suggesting that reduced NADPH oxidase and Rho kinase activity are involved in the improvement of endothelial function induced by microbiota from SHR treated with AML. Similarly, the aortic rings incubated with an antibody neutralizing IL17 also showed improved acetylcholine relaxation in the S-S and S-SHCTZ groups (Figure 9e). These modifications of vascular function were associated with reduced Th17 cell infiltration in the vascular wall (Figure 9f) and lower proportion of Th17 cells in MLNs in S-SAML in comparison with the S-S group (Figure 9g). Additionally, FMT from SHR-AML to SHR incremented colonic mRNA levels of occludin and ZO-1, whereas HCTZ increased MUC-3 expression (Figure 10a). The protein expression of ZO-1 was found higher in S-SAML group as compared to S-S group (Figure 10b). However, we only found reduce plasma LPS in the S-SAML group (Figure 10c), suggesting that microbiota from AML-treated SHR reduced colonic permeability after transplantation to SHR. In addition, lower mRNA levels of the proinflammatory cytokines IL-1ß, and TNF-α were observed in S-SAML in comparison with S-S (Figure 10d), with no change in S-SHCTZ. GPR43 is a key receptor activated by acetate (Marques et al., 2017). We also found increased colonic **GPR43** transcript in the S-SAML group in comparison with the S-S (Figure 10e), suggesting that microbiota from AML-treated SHR induced positive changes in the gut by GPR43 activation. To test if they are a gut-brain communication, as described previously (Toral et al., 2019) we found reduced IL-1ß, and TNF-α levels in PVN from the S-SAML group as compared to the S-S, and being without change in S-SHCTZ (Figure S9a). In agreement with the lower plasma LPS found in S-SAML we also detected reduced TLR4 mRNA levels in PVN (Figure S9b), suggesting that transfer microbiota from SHR treated with AML to SHR lower microglia activation and inflammation.

At the end of the experiment the composition of faecal microbiota was analysed. The bacterial communities evaluated by calculating major ecological parameters, such as Chao richness, and Shannon and Simpson diversity, were different between the S-S and S-SHCTZ groups (Figure S10a). Moreover, the bacterial taxa were clearly separated between these two groups, with no perfect clustering between S-S and S-SAML (Figure S10b). The analysis of the phyla composition showed a profound reduction in the implantation of Firmicutes and increased abundance of Bacteroidetes, as compared with the

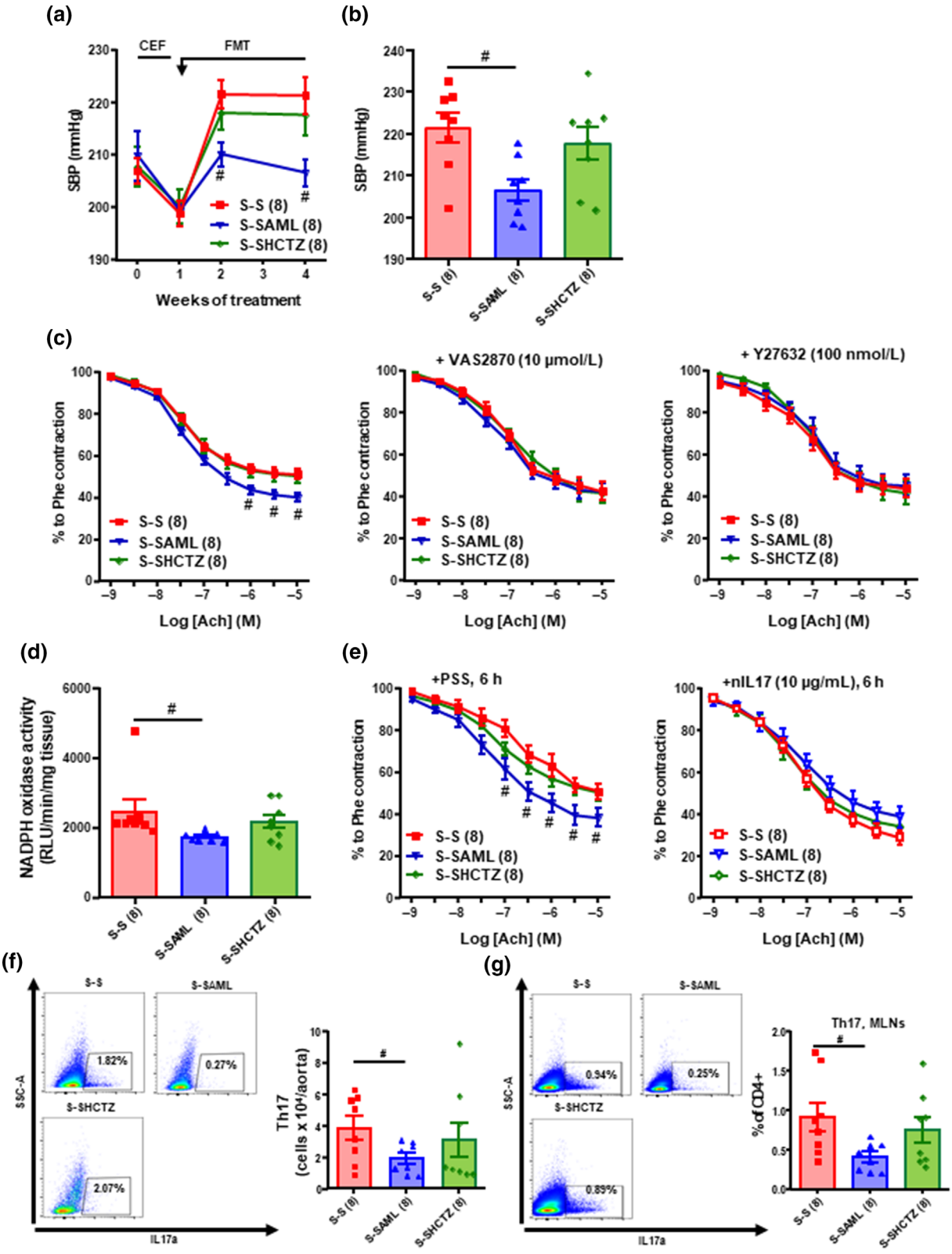

FIGURE 9 Legend on next page.

transplanted microbiota. No significant changes in the relative abundance of phyla among all experimental groups were found (Figure S10c). Interestingly, the relative proportion of the family *S24_7* was increased in the S-SAML group compared with S-S (Figure S10d). There is a strong negative correlation between the abundance of this family and SBP (Figure S10e).

4 | DISCUSSION

As we showed above, a crucial discovery made from our experiments is that the antihypertensive effects of the first-line antihypertensive drugs examined in this study are linked to an improvement in gut dysbiosis and general gut pathology in SHR, except in the case of HCTZ. Proving this point, captopril and AML: (1) attenuated gut leakiness and wall pathology; (ii) reshaped colonic α-defensin production; (iii) increased the relative abundance of strict anaerobic bacteria and acetate-producing bacteria, bacterial communities associated with normal BP; (iv) attenuated neuroinflammation in PVN; (v) dampened gut sympathetic activity; and (vi) microbiota treated with AML transferred, at least in part, their BP lowering effect, and the vasculoprotective, immunomodulatory and anti-neuroinflammatory effects, reshaping recipient gut microbiota with a higher proportion of bacteria belonging to family *S24_7*. By contrast, HCTZ was unable to reduce neuroinflammation, gut sympathetic drive, gut pathology, and permeability, but changed the gut microbiota, decreasing the F/B ratio, and increasing the population of strict anaerobic bacteria. However, microbiome changes induced by HCTZ, with reduced butyrate-producing bacteria, were unable to transfer the antihypertensive phenotype. Therefore, the beneficial effects of AML could, partially, derive from its influence on the brain-gut-vascular wall axis. Interestingly, captopril and HCTZ also induced changes in gut microbiota composition in control WKY rats.

Recently, a notable amount of evidence is beginning to suggest that there is an association between hypertension and intestinal dysbiosis. This connection has been found both in patients and in a wide variety of experimental models of hypertension (Marques et al., 2017; Robles-Vera et al., 2018, 2020,b,c, 2021; Toral et al., 2019; Xia et al., 2021; Yang et al., 2015, 2019). Our present results agree partially with the key known characteristics of dysbiosis seen elsewhere in SHR (Robles-Vera et al., 2020,c, 2021; Toral et al., 2019; Xia et al., 2021; Yang et al., 2015), such as a reduction in acetate-producing bacteria and in strict anaerobic bacteria with a higher proportion of strict aerobic bacteria. All first-line antihypertensive drugs used in this study changed microbiota composition in SHR. The observed effect of these drugs on the microbiota could be due to various mechanisms. Shifts in the composition of the gut microbiota can be associated with changes in the health of the host. Thus, modulating the microbiota could result in a reduction in BP, by shifting its composition to those detected in healthy control subjects. Nevertheless, our group has already shown that hydralazine is able to normalize BP in hypertensive rats without changes in the composition of the gut microbiota (Robles-Vera, Toral, de la Visitación, Sánchez, Gómez-Guzmán, Muñoz, et al., 2020), showing that a return to a microbiota similar to the one in normotensive rats is not a necessary part of the mechanism. In agreement with this, HCTZ reduced BP to a similar extent as AML, but the changes induced by these agents in the microbiota composition are quite different. Shifts in the composition of the gut microbiota have been linked to gut integrity (Kim et al., 2018; Robles-Vera, Toral, de la Visitación, Sánchez, Gómez-Guzmán, Muñoz, et al., 2020; Xiong et al., 2023). Here we show that there exists a pathological state in the gut of hypertensive rats, including an increase in fibrosis, muscular tissue and leakiness and permeability.

Moreover, we detected stunted villi and a reduction in goblet cells in hypertensive rats. The intestinal epithelium creates a tight barrier that contributes to the characteristic hypoxia of the gut lumen. When this tissue gets damaged, it results in an increase in oxygen availability, which favours the growth of aerobic bacteria (Earley et al., 2015). SHR rats present a decrease in the tight junction proteins occludin and ZO-1, which were localized on the peripheral membrane of epithelial cells, and both being normalized by the captopril and AML treatments. Surprisingly, HCTZ increased the relative abundance of strict anaerobic bacteria (mainly *Barnesiella*), but it was unable to restore gut integrity, suggesting the involvement of other mechanisms in the changes induced by HCTZ in the microbiota. Previous studies indicated antibiotic activity by sulphonamide diuretics, such as HCTZ, by bacterial dihydrofolate reductase inhibition (Kaur et al., 2020). This effect is believed to expand butyrate producing taxa of the gut microbiome, which in turn supports good health (Maniar et al., 2017). However, in the gut hypertensive environment HCTZ reduced the populations of butyrate-producing bacteria from the *Lachnospiraceae* family, and in normotensive WKY rats also reduced the proportion of *Coprococcus* (*Lachnospiraceae*). In contrast, the changes in gut microbiota caused by AML were almost entirely specific to a hypertensive environment, as only minor changes were observed in WKY rats. High intestinal permeability in adult hypertensive SHR also presents an

FIGURE 9 Effects of faecal microbiota transplantation from spontaneously hypertensive rat (SHR)-amlodipine (AML) and SHR-hydrochlorothiazide (HCTZ) to control SHR on vascular function in control SHR. (a) Time course of systolic BP (SBP), and final SBP (b) measured by tail-cuff plethysmography, in SHR with stool transplant from SHR (S-S) or from SHR treated with AML (S-SAML) or with HCTZ (S-SHCTZ). (c) Endothelium-dependent relaxation induced by acetylcholine (Ach) in aortas pre-contracted by phenylephrine in the absence or in the presence of VAS2870 or Y27632 for 30 min. (d) NADPH oxidase activity measured by lucigenin-enhanced chemiluminescence in aorta from all experimental groups. (e) Endothelium-dependent relaxation induced by Ach in aortas pre-contracted by phenylephrine (phe) after 6 h of incubation with physiological saline solution (PSS) or with IL-17a neutralizing antibody (nIL17). (f) T helper (Th)17 infiltration in aorta, and (g) Th17 population in mesenteric lymph nodes (MLNs) from all experimental groups measured by flow cytometry. Values are represented as mean ± SEM. The number of animals analysed is shown in parenthesis. # indicates $P < 0.05$ compared with the S-S group.

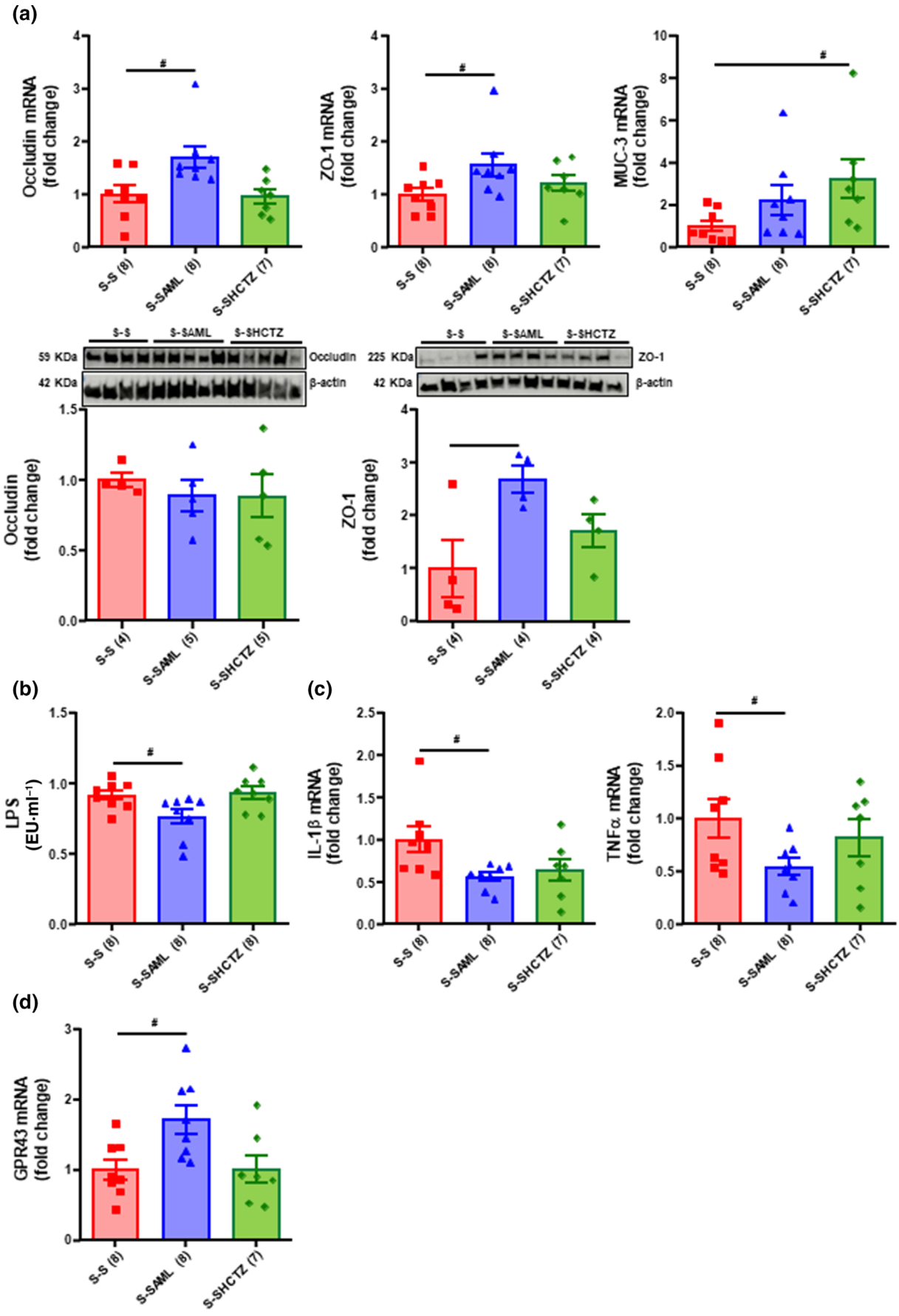

FIGURE 10 Legend on next page.

association with reduced goblet cells, and mucins (Santisteban et al., 2017). HCTZ increased colonic goblet cells and increased mRNA levels of MUC-3, but it was unable to reduce marker of gut permeability, such as plasma levels of LPS and FABP2. Moreover, the cells that form the intestinal epithelium and Paneth cells secrete antimicrobial peptides (eg. defensins) that selectively target Gram-positive bacteria to cause their depletion (Ayabe et al., 2000; Pamer, 2007; Vaishnava et al., 2008; Vora et al., 2004). Our group observed changes in α-defensin levels in colon from SHR compared to WKY, which might also be involved in changes in the SHR microbiota. These changes were normalized by both captopril and AML treatments and might contribute to reshaping the gut microbiota. However, the changes induced by HCTZ in the gut microbiota were independent of α-defensin production.

Mounting evidence suggests that an activated microglia–neuron unit in the PVN can increase gut sympathetic drive; this is associated with more severe gut pathology and inflammatory status, and gut dysbiosis and permeability, pointing to a brain-gut axis driven by the sympathetic response (Santisteban et al., 2017; Sharma et al., 2019; Toral et al., 2019; Zubcevic et al., 2019). Actually, the inhibition of microglial activation and neuroinflammation by intracerebroventricular administration of a modified **tetracycline** normalizes the sympathetic activity, producing shifts in the gut microbiota and the amelioration of gut pathology (Sharma et al., 2019). In agreement with these data, we observed in PVN from SHR a higher number of microglia cells than in the WKY group, which was reduced by captopril. However, in agreement with previous data, ACE inhibition with captopril (Richards et al., 2022) or L-type Ca^{2+} channel blockade with AML (Huang et al., 2014; Kim et al., 2022) normalized the mRNA levels of higher pro-inflammatory cytokines (TNF-α, IL-1β, and IL-6). These protective effects could be partially related to a reduced proinflammatory TLR4 pathway in PVN. Furthermore, activation of PVN AT_1 receptors facilitates the sympathetic outflow, increasing the NADPH oxidase-dependent ROS production (Gao et al., 2005). As expected, captopril and AML, but not HCTZ, reduced NADPH oxidase-driven ROS production in PVN and reduced sympathetic excitation (less BP reduction after nicotinic blockade, and lower plasma NA levels).

Our present data suggest a high gut sympathetic drive (indicated by an increase in tyrosine hydroxylase and NA levels), which is linked to microbial dysbiosis and decreased gut integrity in hypertensive animals. These findings agree with those of Santisteban et al. (2017). Several authors have already shown that a reduction of sympathetic activity in the colon induced by captopril (Santisteban et al., 2017), losartan (Robles-Vera, Toral, de la Visitación, Sánchez, Gómez-Guzmán, Muñoz, et al., 2020) or spironolactone (González-Correa et al., 2023) ameliorated gut pathology and reduced gut dysbiosis, while hydralazine (which increases gut sympathetic drive) was incapable of normalizing gut integrity and microbiota composition (Robles-Vera, Toral, de la Visitación, Sánchez, Gómez-Guzmán, Muñoz, et al., 2020). We observed an increase in mRNA levels of tyrosine hydroxylase and in NA content in the SHR colon, which were restored by both captopril and AML, but not by HCTZ. Thus, captopril and AML in SHR decreased the sympathetic excitation, inducing a low gut sympathetic drive that improves gut pathology and gut dysbiosis in SHR.

It is known that, through modulation of the immune system and gut-brain communication, the microbiota is able to reduce BP (Robles-Vera, Toral, & Duarte, 2020). Karbach et al. (2016) demonstrated that angiotensin II infusion to germ-free mice decreased ROS formation in the vascular system, attenuating Nox2 activity, a subunit of NADPH oxidase, and decreased up-regulation of RORγ, the signature transcription factor for IL-17 synthesis in aorta. The aforementioned effects conferred protection from endothelial dysfunction and attenuated the increase in BP in response to angiotensin II, involving the immune system in the vascular effects of the microbiota. In a previous article, we showed that FMT from SHR treated with losartan to SHR decreased BP, ameliorated endothelial dysfunction, and the aortic NADPH oxidase activity associated with high aortic Tregs infiltration (Robles-Vera, Toral, de la Visitación, Sánchez, Gómez-Guzmán, Muñoz, et al., 2020). When we explore the effects of FMT from donor SHR-HCTZ, SHR-AML or untreated-SHR to receptor SHR, we found that microbiota from AML-treated rats reduced BP and exerted vascular protection from oxidative stress as compared to FMT from untreated SHR, whereas those treated with HCTZ were without protective effects. The donor microbiota from SHR-AML have a higher proportion of acetate-producing bacteria than untreated SHR, whereas those from SHR-HCTZ showed similar acetate-and lower butyrate-producing bacteria to the SHR-SHR group. SCFAs are relevant metabolites for the maintenance of intestinal homeostasis. SCFAs can act as fuel for intestinal epithelial cells, intervene in the strengthening of the gut barrier function (Parada Venegas et al., 2019) and regulate gut-immune system communication in gut secondary lymph organs (Robles-Vera, Toral, de la Visitación, Sánchez, Gómez-Guzmán, Romero, et al., 2020). The protective effects on gut integrity and permeability induced by microbiota from SHR-AML are linked with acetate-GPR43 pathway. Moreover, reduced CD4+ polarization to proinflammatory Th17 cells in MLNs and lower Th17 infiltration in the vascular wall are involved in the improvement of endothelial dysfunction. We also previously found that microbiota

FIGURE 10 Effects of faecal microbiota transplantation from spontaneously hypertensive rat (SHR)-amlodipine (AML) and SHR-hydrochlorothiazide (HCTZ) to control SHR on the gut integrity, permeability, and inflammation. (a) mRNA levels of occludin, zonula occludens-1 (ZO-1) and mucin (MUC)-3 in the colon in all experimental groups. Where n<5, statistical tests were not carried out, and these data can be regarded as preliminary. (b) Protein expression of occludin and ZO-1 analysed by western blots and normalized to β-actin expression in the colon in all experimental groups. Protein of interest and β-actin were analysed in the same membranes. (C) Levels of plasma endotoxin (endotoxin units per millilitre [EU·ml^{-1}]). (d) mRNA levels of pro-inflammatory cytokines, interleukin IL-1β and tumour necrosis factor α (TNFα) and (e) GPR43 in colonic samples. Values are represented as mean ± SEM. The number of animals analysed is shown in parenthesis. $^{\#}$ indicates $P < 0.05$ compared with the S-S group.

transplants from normotensive WKY rats to SHR decreased neuroinflammation and sympathetic drive (Toral et al., 2019). Moreover, the antihypertensive effects of the ACE inhibitor captopril holds a continued influence on the brain-gut axis even after treatment withdrawal (Yang et al., 2019). Interestingly, in this study we also found lower neuroinflammation in the S-SAML group as compared to S-S, associated with lower plasma LPS and its target receptor TLR4 in PVN, suggesting improvement of the gut-brain axis induced by AML, whereas microbiome changes induced by HCTZ did not influence the communication between gut and brain.

When gut microbiota is transplanted, a cross-interaction is established between the microbiota and the host, which can lead to changes in its composition to adapt to the conditions of the gut environment, but also to alter the pathological state of the host despite the complexity of arterial hypertension in this genetic model. A significant increase in the relative abundance of bacteria belonging to family *S24_7* was found in faeces from SHR transplanted with donor microbiota from SHR treated with AML, which correlates with reduced BP. A higher proportion of this family correlated positively with splenic FoxP3+ CD4+ Treg cells and delayed diabetes onset age (Krych et al., 2015), with increased inner mucus layer barrier function (Volk et al., 2019), and with the lower BP induced by probiotics and SCFAs in SHR (Robles-Vera, Toral, de la Visitación, Sánchez, Gómez-Guzmán, Romero, et al., 2020). However, whether bacteria belonging to *S24_7* are responsible for reduced BP induced by AML deserves further investigation.

There are some limitations in our study. First, the impact of environmental factors that vary among animal facilities, including housing conditions (ambient temperature, humidity), and the chow composition used in the present experiment, as compared with previous studies (Robles-Vera, Toral, de la Visitación, Sánchez, Gómez-Guzmán, Muñoz, et al., 2020), could modify gut microbiota composition, potentially affecting the BP effects of these drugs. Second, the lack of specificity in the ROS detection assays used was partially addressed following the American Heart Association recommendations, which suggest that the best practice to confirm findings is to use more than one assay and include appropriate controls (Griendling et al., 2016). Third, considering the clear differences between the composition of transplanted and implanted microbiota in SHR, the conclusions of the FMT study must be interpreted with caution.

In conclusion, we have found for the first time that first-line antihypertensive drugs changed gut dysbiosis in SHR. The effects of captopril and AML could be associated with their capability to decrease neuroinflammation and the subsequent sympathetic drive in the gut, ameliorating gut integrity and defensin production, whereas HCTZ treatment was without these effects. AML-induced changes in the gut microbiota might contribute, at least partially, to the protection of the vasculature and the reduction in BP, possibly by modulating the gut immune system and the gut-brain axis. However, further investigation is needed to verify the precise mechanisms of AML-induced changes in gut microbiota and its communication with immune system and brain.

AUTHOR CONTRIBUTIONS

J. Duarte conceived and designed the research; C. González-Correa, J. Moleón, S. Miñano, I. Robles-Vera, M. Toral, A. M. Barranco, N. Martín-Morales, F. O'Valle, M. Sánchez, M. Gómez-Guzmán, E. Guerra-Hernández and M. Romero performed the experiments and analysed the data; R. Jiménez and J. Duarte interpreted the results; C. González-Correa, J. Moleón, S. Miñano, M. Sánchez and R. Jiménez prepared figures; M. Romero and J. Duarte drafted this manuscript; I. Robles-Vera, M. Toral, M. Gómez-Guzmán, M. Romero and J. Duarte edited and revised the manuscript. All authors approved the final version of manuscript. All authors approved the final version of manuscript.

ACKNOWLEDGEMENTS

This work was supported by Grants from Agencia Estatal de Investigación (AEI), Ministerio de Ciencia e Innovación (MCIN) (PID2020-116347RB-I00 funded by MCIN/AEI/10.13039/501100011033) and Junta de Andalucía (CTS 164, P20_00193 and A-CTS-318-UGR20) with funds from the European Union and by the Ministerio de Economia y Competitividad, Instituto de Salud Carlos III (CIBER-CV), Spain. M.T. and I.R.-V. are postdoctoral fellow of Spanish Ministerio de Ciencia e Innovación (Juan de la Cierva Incorporación Program, IJC2020-044581-I, and Juan de la Cierva Formación Program, respectively). J. M. is a predoctoral fellow of MCIN, and C. G.-C. and S. M. are predoctoral fellow of Junta de Andalucía. The cost of this publication was paid in part with funds from the European Union (Fondo Europeo de Desarrollo Regional, FEDER, 'FEDER una manera de hacer Europa').

CONFLICT OF INTEREST STATEMENT

The authors declare no conflict of interest.

DATA AVAILABILITY STATEMENT

Data are available on request from the authors. The data that support the findings of this study are available from the corresponding author upon reasonable request. Some data may not be made available because of privacy or ethical restrictions.

DECLARATION OF TRANSPARENCY AND SCIENTIFIC RIGOUR

This Declaration acknowledges that this paper adheres to the principles for transparent reporting and scientific rigour of preclinical research as stated in the *BJP* guidelines for Design & Analysis, Immunoblotting and Immunochemistry and Animal Experimentation, and as recommended by funding agencies, publishers and other organizations engaged with supporting research.

ORCID

Javier Moleón https://orcid.org/0000-0003-4447-696X
Marta Toral https://orcid.org/0000-0001-5324-8569
Manuel Gómez-Guzmán https://orcid.org/0000-0003-2452-9286

REFERENCES

Alexander, S. P. H., Christopoulos, A., Davenport, A. P., Kelly, E., Mathie, A. A., Peters, J. A., Veale, E. L., Armstrong, J. F., Faccenda, E., Harding, S. D., Davies, J. A., Abbracchio, M. P., Abraham, G., Agoulnik, A., Alexander, W., al-hosaini, K., Bäck, M., Baker, J. G., Barnes, N. M., … Ye, R. D. (2023). The Concise Guide to PHARMACOLOGY 2023/24: G protein-coupled receptors. *British Journal of Pharmacology*, *180*, S23–S144. https://doi.org/10.1111/bph.16177

Alexander, S. P. H., Fabbro, D., Kelly, E., Mathie, A. A., Peters, J. A., Veale, E. L., Armstrong, J. F., Faccenda, E., Harding, S. D., Davies, J. A., Annett, S., Boison, D., Burns, K. E., Dessauer, C., Gertsch, J., Helsby, N. A., Izzo, A. A., Ostrom, R., Papapetropoulos, A., … Wong, S. S. (2023). The Concise Guide to PHARMACOLOGY 2023/24: Enzymes. *British Journal of Pharmacology*, *180*, S289–S373. https://doi.org/10.1111/bph.16181

Alexander, S. P. H., Fabbro, D., Kelly, E., Mathie, A. A., Peters, J. A., Veale, E. L., Armstrong, J. F., Faccenda, E., Harding, S. D., Davies, J. A., Beuve, A., Brouckaert, P., Bryant, C., Burnett, J. C., Farndale, R. W., Friebe, A., Garthwaite, J., Hobbs, A. J., Jarvis, G. E., … Waldman, S. A. (2023). The Concise Guide to PHARMACOLOGY 2023/24: Catalytic receptors. *British Journal of Pharmacology*, *180*, S241–S288. https://doi.org/10.1111/bph.16180

Alexander, S. P. H., Kelly, E., Mathie, A. A., Peters, J. A., Veale, E. L., Armstrong, J. F., Buneman, O. P., Faccenda, E., Harding, S. D., Spedding, M., Cidlowski, J. A., Fabbro, D., Davenport, A. P., Striessnig, J., Davies, J. A., Ahlers-Dannen, K. E., Alqinyah, M., Arumugam, T. V., Bodle, C., … Zolghadri, Y. (2023). The Concise Guide to PHARMACOLOGY 2023/24: Introduction and Other Protein Targets. *British Journal of Pharmacology*, *180*, S1–S22. https://doi.org/10.1111/bph.16176

Alexander, S. P. H., Roberts, R. E., Broughton, B. R. S., Sobey, C. G., George, C. H., Stanford, S. C., Cirino, G., Docherty, J. R., Giembycz, M. A., Hoyer, D., Insel, P. A., Izzo, A. A., Ji, Y., MacEwan, D. J., Mangum, J., Wonnacott, S., & Ahluwalia, A. (2018). Goals and practicalities of immunoblotting and immunohistochemistry: A guide for submission to the British Journal of pharmacology. *British Journal of Pharmacology*, *175*(3), 407–411. https://doi.org/10.1111/bph.14112

Ayabe, T., Satchell, D. P., Wilson, C. L., Parks, W. C., Selsted, M. E., & Ouellette, A. J. (2000). Secretion of microbicidal alpha-defensins by intestinal Paneth cells in response to bacteria. *Nature Immunology*, *1*(2), 113–118. https://doi.org/10.1038/77783

Bevins, C. L. (2005). Events at the host-microbial interface of the gastrointestinal tract. V. Paneth cell alpha-defensins in intestinal host defense. *American Journal of Physiology. Gastrointestinal and Liver Physiology*, *289*(2), G173–G176. https://doi.org/10.1152/ajpgi.00079.2005

Chong, J., Liu, P., Zhou, G., & Xia, J. (2020). Using MicrobiomeAnalyst for comprehensive statistical, functional, and meta-analysis of microbiome data. *Nature Protocols*, *15*(3), 799–821. https://doi.org/10.1038/s41596-019-0264-1

Curtis, M. J., Alexander, S. P. H., Cirino, G., George, C. H., Kendall, D. A., Insel, P. A., Izzo, A. A., Ji, Y., Panettieri, R. A., Patel, H. H., Sobey, C. G., Stanford, S. C., Stanley, P., Stefanska, B., Stephens, G. J., Teixeira, M. M., Vergnolle, N., & Ahluwalia, A. (2022). Planning experiments: Updated guidance on experimental design and analysis and their reporting III. *British Journal of Pharmacology*, *179*(15), 3907–3913. https://doi.org/10.1111/bph.15868

Dange, R. B., Agarwal, D., Teruyama, R., & Francis, J. (2015). Toll-like receptor 4 inhibition within the paraventricular nucleus attenuates blood pressure and inflammatory response in a genetic model of hypertension. *Journal of Neuroinflammation*, *12*, 31. https://doi.org/10.1186/s12974-015-0242-7

Doggrell, S. A., & Brown, L. (1998). Rat models of hypertension, cardiac hypertrophy and failure. *Cardiovascular Research*, *39*(1), 89–105. https://doi.org/10.1016/s0008-6363(98)00076-5

Earley, Z. M., Akhtar, S., Green, S. J., Naqib, A., Khan, O., Cannon, A. R., Hammer, A. M., Morris, N. L., Li, X., Eberhardt, J. M., Gamelli, R. L., Kennedy, R. H., & Choudhry, M. A. (2015). Burn injury alters the intestinal microbiome and increases gut permeability and bacterial translocation. *PLoS ONE*, *10*(7), e0129996. https://doi.org/10.1371/journal.pone.0129996

Forslund, S. K., Chakaroun, R., Zimmermann-Kogadeeva, M., Markó, L., Aron-Wisnewsky, J., Nielsen, T., Moitinho-Silva, L., Schmidt, T. S. B., Falony, G., Vieira-Silva, S., Adriouch, S., Alves, R. J., Assmann, K., Bastard, J. P., Birkner, T., Caesar, R., Chilloux, J., Coelho, L. P., Fezeu, L., … Bork, P. (2021). Combinatorial, additive and dose-dependent drug-microbiome associations. *Nature*, *600*(7889), 500–505. https://doi.org/10.1038/s41586-021-04177-9

Gao, L., Wang, W., Li, Y. L., Schultz, H. D., Liu, D., Cornish, K. G., & Zucker, I. H. (2005). Sympathoexcitation by central ANG II: Roles for AT1 receptor upregulation and NAD(P)H oxidase in RVLM. *American Journal of Physiology. Heart and Circulatory Physiology*, *288*(5), H2271–H2279. https://doi.org/10.1152/ajpheart.00949.2004

Gómez-Guzmán, M., Jiménez, R., Sánchez, M., Romero, M., O'Valle, F., Lopez-Sepulveda, R., Quintela, A. M., Galindo, P., Zarzuelo, M. J., Bailón, E., Delpón, E., Perez-Vizcaino, F., & Duarte, J. (2011). Chronic (−)-epicatechin improves vascular oxidative and inflammatory status but not hypertension in chronic nitric oxide-deficient rats. *The British Journal of Nutrition*, *106*(9), 1337–1348. https://doi.org/10.1017/S0007114511004314

González-Correa, C., Moleón, J., Miñano, S., Robles-Vera, I., Toral, M., Martín-Morales, N., O'Valle, F., Sánchez, M., Gómez-Guzmán, M., Jiménez, R., Romero, M., & Duarte, J. (2023). Mineralocorticoid receptor blockade improved gut microbiota dysbiosis by reducing gut sympathetic tone in spontaneously hypertensive rats. *Biomedicine & Pharmacotherapy = Biomedecine & Pharmacotherapie*, *158*, 114149. https://doi.org/10.1016/j.biopha.2022.114149

Griendling, K. K., Touyz, R. M., Zweier, J. L., Dikalov, S., Chilian, W., Chen, Y. R., Harrison, D. G., Bhatnagar, A., & American Heart Association Council on Basic Cardiovascular Sciences. (2016). Measurement of reactive oxygen species, reactive nitrogen species, and redox-dependent signaling in the cardiovascular system: A scientific Statement from the American Heart Association. *Circulation Research*, *119*(5), e39–e75. https://doi.org/10.1161/RES.0000000000000110

Guzik, T. J., Hoch, N. E., Brown, K. A., McCann, L. A., Rahman, A., Dikalov, S., Goronzy, J., Weyand, C., & Harrison, D. G. (2007). Role of the T cell in the genesis of angiotensin II induced hypertension and vascular dysfunction. *The Journal of Experimental Medicine*, *204*(10), 2449–2460. https://doi.org/10.1084/jem.20070657

Hashimoto, T., Perlot, T., Rehman, A., Trichereau, J., Ishiguro, H., Paolino, M., Sigl, V., Hanada, T., Hanada, R., Lipinski, S., Wild, B., Camargo, S. M., Singer, D., Richter, A., Kuba, K., Fukamizu, A., Schreiber, S., Clevers, H., Verrey, F., … Penninger, J. M. (2012). ACE2 links amino acid malnutrition to microbial ecology and intestinal inflammation. *Nature*, *487*(7408), 477–481. https://doi.org/10.1038/nature11228

Huang, B. R., Chang, P. C., Yeh, W. L., Lee, C. H., Tsai, C. F., Lin, C., Lin, H. Y., Liu, Y. S., Wu, C. Y., Ko, P. Y., Huang, S. S., Hsu, H. C., & Lu, D. Y. (2014). Anti-neuroinflammatory effects of the calcium channel blocker nicardipine on microglial cells: Implications for neuroprotection. *PLoS ONE*, *9*(3), e91167. https://doi.org/10.1371/journal.pone.0091167

Karbach, S. H., Schönfelder, T., Brandão, I., Wilms, E., Hörmann, N., Jäckel, S., Schüler, R., Finger, S., Knorr, M., Lagrange, J., Brandt, M., Waisman, A., Kossmann, S., Schäfer, K., Münzel, T., Reinhardt, C., & Wenzel, P. (2016). Gut microbiota promote angiotensin II-induced arterial hypertension and vascular dysfunction. *Journal of the American Heart Association*, *5*(9), e003698. https://doi.org/10.1161/JAHA.116.003698

Kaur, S., Bhattacharyya, R., & Banerjee, D. (2020). Hydrochlorothiazide and Indapamide bind the NADPH binding site of bacterial Dihydrofolate reductase: Results of an in-silico study and their implications. *In Silico Pharmacology*, *8*(1), 5. https://doi.org/10.1007/s40203-020-00056-9

Kim, J., Jeon, S. G., Jeong, H. R., Park, H., Kim, J. I., & Hoe, H. S. (2022). L-type Ca^{2+} channel inhibition rescues the LPS-induced Neuroinflammatory response and impairments in spatial memory and dendritic spine formation. *International Journal of Molecular Sciences*, *23*(21), 13606. https://doi.org/10.3390/ijms232113606

Kim, S., Goel, R., Kumar, A., Qi, Y., Lobaton, G., Hosaka, K., Mohammed, M., Handberg, E. M., Richards, E. M., Pepine, C. J., & Raizada, M. K. (2018). Imbalance of gut microbiome and intestinal epithelial barrier dysfunction in patients with high blood pressure. *Clinical Science (London, England : 1979)*, *132*(6), 701–718. https://doi.org/10.1042/CS20180087

Krych, Ł., Nielsen, D. S., Hansen, A. K., & Hansen, C. H. (2015). Gut microbial markers are associated with diabetes onset, regulatory imbalance, and IFN-γ level in NOD mice. *Gut Microbes*, *6*(2), 101–109. https://doi.org/10.1080/19490976.2015.1011876

Li, J., Zhao, F., Wang, Y., Chen, J., Tao, J., Tian, G., Wu, S., Liu, W., Cui, Q., Geng, B., Zhang, W., Weldon, R., Auguste, K., Yang, L., Liu, X., Chen, L., Yang, X., Zhu, B., & Cai, J. (2017). Gut microbiota dysbiosis contributes to the development of hypertension. *Microbiome*, *5*(1), 14. https://doi.org/10.1186/s40168-016-0222-x

Lilley, E., Stanford, S. C., Kendall, D. E., Alexander, S. P. H., Cirino, G., Docherty, J. R., George, C. H., Insel, P. A., Izzo, A. A., Ji, Y., Panettieri, R. A., Sobey, C. G., Stefanska, B., Stephens, G., Teixeira, M., & Ahluwalia, A. (2020). ARRIVE 2.0 and the British Journal of pharmacology: Updated guidance for 2020. *British Journal of Pharmacology*, *177*(16), 3611–3616. https://doi.org/10.1111/bph.15178

Liu, G., Cheng, J., Zhang, T., Shao, Y., Chen, X., Han, L., Zhou, R., & Wu, B. (2022). Inhibition of microbiota-dependent trimethylamine N-oxide production ameliorates high salt diet-induced sympathetic excitation and hypertension in rats by attenuating central Neuroinflammation and oxidative stress. *Frontiers in Pharmacology*, *13*, 856914. https://doi.org/10.3389/fphar.2022.856914

Maier, L., Pruteanu, M., Kuhn, M., Zeller, G., Telzerow, A., Anderson, E. E., Brochado, A. R., Fernandez, K. C., Dose, H., Mori, H., Patil, K. R., Bork, P., & Typas, A. (2018). Extensive impact of non-antibiotic drugs on human gut bacteria. *Nature*, *555*(7698), 623–628. https://doi.org/10.1038/nature25979

Maniar, K., Moideen, A., Mittal, A., Patil, A., Chakrabarti, A., & Banerjee, D. (2017). A story of metformin-butyrate synergism to control various pathological conditions as a consequence of gut microbiome modification: Genesis of a wonder drug? *Pharmacological Research*, *117*, 103–128. https://doi.org/10.1016/j.phrs.2016.12.003

Marques, F. Z., Nelson, E., Chu, P. Y., Horlock, D., Fiedler, A., Ziemann, M., Tan, J. K., Kuruppu, S., Rajapakse, N. W., El-Osta, A., Mackay, C. R., & Kaye, D. M. (2017). High-fiber diet and acetate supplementation change the gut microbiota and prevent the development of hypertension and heart failure in hypertensive mice. *Circulation*, *135*(10), 964–977. https://doi.org/10.1161/CIRCULATIONAHA.116.024545

Mowat, A. M., & Agace, W. W. (2014). Regional specialization within the intestinal immune system. *Nature Reviews. Immunology*, *14*(10), 667–685. https://doi.org/10.1038/nri3738

Muralitharan, R. R., Jama, H. A., Xie, L., Peh, A., Snelson, M., & Marques, F. Z. (2020). Microbial peer pressure: The role of the gut microbiota in hypertension and its complications. *Hypertension (Dallas, Tex. : 1979)*, *76*(6), 1674–1687. https://doi.org/10.1161/HYPERTENSIONAHA.120.14473

Niess, J. H., Brand, S., Gu, X., Landsman, L., Jung, S., McCormick, B. A., Vyas, J. M., Boes, M., Ploegh, H. L., Fox, J. G., Littman, D. R., & Reinecker, H. C. (2005). CX3CR1-mediated dendritic cell access to the intestinal lumen and bacterial clearance. *Science (New York, N.Y.)*, *307*(5707), 254–258. https://doi.org/10.1126/science.1102901

Nishihara, M., Hirooka, Y., Kishi, T., & Sunagawa, K. (2012). Different role of oxidative stress in paraventricular nucleus and rostral ventrolateral medulla in cardiovascular regulation in awake spontaneously hypertensive rats. *Journal of Hypertension*, *30*(9), 1758–1765. https://doi.org/10.1097/HJH.0b013e32835613d7

Pamer, E. G. (2007). Immune responses to commensal and environmental microbes. *Nature Immunology*, *8*(11), 1173–1178. https://doi.org/10.1038/ni1526

Parada Venegas, D., De la Fuente, M. K., Landskron, G., González, M. J., Quera, R., Dijkstra, G., Harmsen, H. J. M., Faber, K. N., & Hermoso, M. A. (2019). Corrigendum: Short chain fatty acids (SCFAs)-mediated gut epithelial and immune regulation and its relevance for inflammatory bowel diseases. *Frontiers in Immunology*, *10*, 1486. https://doi.org/10.3389/fimmu.2019.01486

Percie du Sert, N., Hurst, V., Ahluwalia, A., Alam, S., Avey, M. T., Baker, M., Browne, W. J., Clark, A., Cuthill, I. C., Dirnagl, U., Emerson, M., Garner, P., Holgate, S. T., Howells, D. W., Karp, N. A., Lazic, S. E., Lidster, K., MacCallum, C. J., Macleod, M., … Würbel, H. (2020). The ARRIVE guidelines 2.0: Updated guidelines for reporting animal research. *PLoS Biology*, *18*(7), e3000410. https://doi.org/10.1371/journal.pbio.3000410

Richards, E. M., Li, J., Stevens, B. R., Pepine, C. J., & Raizada, M. K. (2022). Gut microbiome and Neuroinflammation in hypertension. *Circulation Research*, *130*(3), 401–417. https://doi.org/10.1161/CIRCRESAHA.121.319816

Robles-Vera, I., de la Visitación, N., Toral, M., Sánchez, M., Gómez-Guzmán, M., Jiménez, R., Romero, M., & Duarte, J. (2021). Mycophenolate mediated remodeling of gut microbiota and improvement of gut-brain axis in spontaneously hypertensive rats. *Biomedicine & Pharmacotherapy = Biomedecine & Pharmacotherapie*, *135*, 111189. https://doi.org/10.1016/j.biopha.2020.111189

Robles-Vera, I., de la Visitación, N., Toral, M., Sánchez, M., Romero, M., Gómez-Guzmán, M., Yang, T., Izquierdo-García, J. L., Guerra-Hernández, E., Ruiz-Cabello, J., Raizada, M. K., Pérez-Vizcaíno, F., Jiménez, R., & Duarte, J. (2020). Probiotic Bifidobacterium breve prevents DOCA-salt hypertension. *FASEB Journal : Official Publication of the Federation of American Societies for Experimental Biology*, *34*(10), 13626–13640. https://doi.org/10.1096/fj.202001532R

Robles-Vera, I., Toral, M., de la Visitación, N., Sánchez, M., Gómez-Guzmán, M., Muñoz, R., Algieri, F., Vezza, T., Jiménez, R., Gálvez, J., Romero, M., Redondo, J. M., & Duarte, J. (2020). Changes to the gut microbiota induced by losartan contributes to its antihypertensive effects. *British Journal of Pharmacology*, *177*(9), 2006–2023. https://doi.org/10.1111/bph.14965

Robles-Vera, I., Toral, M., de la Visitación, N., Sánchez, M., Gómez-Guzmán, M., Romero, M., Yang, T., Izquierdo-Garcia, J. L., Jiménez, R., Ruiz-Cabello, J., Guerra-Hernández, E., Raizada, M. K., Pérez-Vizcaíno, F., & Duarte, J. (2020). Probiotics prevent Dysbiosis and the rise in blood pressure in genetic hypertension: Role of short-chain fatty acids. *Molecular Nutrition & Food Research*, *64*(6), e1900616. https://doi.org/10.1002/mnfr.201900616

Robles-Vera, I., Toral, M., de la Visitación, N., Sánchez, M., Romero, M., Olivares, M., Jiménez, R., & Duarte, J. (2018). The probiotic lactobacillus fermentum prevents Dysbiosis and vascular oxidative stress in rats with hypertension induced by chronic nitric oxide blockade. *Molecular Nutrition & Food Research*, *62*(19), e1800298. https://doi.org/10.1002/mnfr.201800298

Robles-Vera, I., Toral, M., & Duarte, J. (2020). Microbiota and hypertension: Role of the sympathetic nervous system and the immune system. *American Journal of Hypertension*, *33*(10), 890–901. https://doi.org/10.1093/ajh/hpaa103

Romero, M., Toral, M., Robles-Vera, I., Sánchez, M., Jiménez, R., O'Valle, F., Rodriguez-Nogales, A., Pérez-Vizcaino, F., Gálvez, J., & Duarte, J.

(2017). Activation of peroxisome proliferator activator receptor β/δ improves endothelial dysfunction and protects kidney in murine lupus. *Hypertension (Dallas, Tex. : 1979)*, *69*(4), 641–650. https://doi.org/10.1161/HYPERTENSIONAHA.116.08655

Sano, T., & Tarazi, R. C. (1987). Differential structural responses of small resistance vessels to antihypertensive therapy. *Circulation*, *75*(3), 618–626. https://doi.org/10.1161/01.cir.75.3.618

Santisteban, M. M., Ahmari, N., Carvajal, J. M., Zingler, M. B., Qi, Y., Kim, S., Joseph, J., Garcia-Pereira, F., Johnson, R. D., Shenoy, V., Raizada, M. K., & Zubcevic, J. (2015). Involvement of bone marrow cells and neuroinflammation in hypertension. *Circulation Research*, *117*(2), 178–191. https://doi.org/10.1161/CIRCRESAHA.117.305853

Santisteban, M. M., Qi, Y., Zubcevic, J., Kim, S., Yang, T., Shenoy, V., Cole-Jeffrey, C. T., Lobaton, G. O., Stewart, D. C., Rubiano, A., Simmons, C. S., Garcia-Pereira, F., Johnson, R. D., Pepine, C. J., & Raizada, M. K. (2017). Hypertension-linked pathophysiological alterations in the gut. *Circulation Research*, *120*(2), 312–323. https://doi.org/10.1161/CIRCRESAHA.116.309006

Sharifi, A. M., Li, J. S., Endemann, D., & Schiffrin, E. L. (1998). Effects of enalapril and amlodipine on small-artery structure and composition, and on endothelial dysfunction in spontaneously hypertensive rats. *Journal of Hypertension*, *16*(4), 457–466. https://doi.org/10.1097/00004872-199816040-00007

Sharma, R. K., Yang, T., Oliveira, A. C., Lobaton, G. O., Aquino, V., Kim, S., Richards, E. M., Pepine, C. J., Sumners, C., & Raizada, M. K. (2019). Microglial cells impact gut microbiota and gut pathology in angiotensin II-induced hypertension. *Circulation Research*, *124*(5), 727–736. https://doi.org/10.1161/CIRCRESAHA.118.313882

Stevens, B. R., Goel, R., Seungbum, K., Richards, E. M., Holbert, R. C., Pepine, C. J., & Raizada, M. K. (2018). Increased human intestinal barrier permeability plasma biomarkers zonulin and FABP2 correlated with plasma LPS and altered gut microbiome in anxiety or depression. *Gut*, *67*(8), 1555–1557. https://doi.org/10.1136/gutjnl-2017-314759

Toral, M., Robles-Vera, I., de la Visitación, N., Romero, M., Yang, T., Sánchez, M., Gómez-Guzmán, M., Jiménez, R., Raizada, M. K., & Duarte, J. (2019). Critical role of the interaction gut microbiota - sympathetic nervous system in the regulation of blood pressure. *Frontiers in Physiology*, *10*, 231. https://doi.org/10.3389/fphys.2019.00231

Touyz, R. M., Rios, F. J., Alves-Lopes, R., Neves, K. B., Camargo, L. L., & Montezano, A. C. (2020). Oxidative stress: A unifying paradigm in hypertension. *The Canadian Journal of Cardiology*, *36*(5), 659–670. https://doi.org/10.1016/j.cjca.2020.02.081

Vaishnava, S., Behrendt, C. L., Ismail, A. S., Eckmann, L., & Hooper, L. V. (2008). Paneth cells directly sense gut commensals and maintain homeostasis at the intestinal host-microbial interface. *Proceedings of the National Academy of Sciences of the United States of America*, *105*(52), 20858–20863. https://doi.org/10.1073/pnas.0808723105

Vera, R., Jiménez, R., Lodi, F., Sánchez, M., Galisteo, M., Zarzuelo, A., Pérez-Vizcaíno, F., & Duarte, J. (2007). Genistein restores caveolin-1 and AT-1 receptor expression and vascular function in large vessels of ovariectomized hypertensive rats. *Menopause (New York, N.Y.)*, *14*(5), 933–940. https://doi.org/10.1097/GME.0b013e31802d9785

Volk, J. K., Nyström, E. E. L., van der Post, S., Abad, B. M., Schroeder, B. O., Johansson, Å., Svensson, F., Jäverfelt, S., Johansson, M. E. V., Hansson, G. C., & Birchenough, G. M. H. (2019). The Nlrp6 inflammasome is not required for baseline colonic inner mucus layer formation or function. *The Journal of Experimental Medicine*, *216*(11), 2602–2618. https://doi.org/10.1084/jem.20190679

Vora, P., Youdim, A., Thomas, L. S., Fukata, M., Tesfay, S. Y., Lukasek, K., Michelsen, K. S., Wada, A., Hirayama, T., Arditi, M., & Abreu, M. T. (2004). Beta-defensin-2 expression is regulated by TLR signaling in intestinal epithelial cells. *Journal of Immunology (Baltimore, Md. : 1950)*, *173*(9), 5398–5405. https://doi.org/10.4049/jimmunol.173.9.5398

Xia, W. J., Xu, M. L., Yu, X. J., Du, M. M., Li, X. H., Yang, T., Li, L., Li, Y., Kang, K. B., Su, Q., Xu, J. X., Shi, X. L., Wang, X. M., Li, H. B., & Kang, Y. M. (2021). Antihypertensive effects of exercise involve reshaping of gut microbiota and improvement of gut-brain axis in spontaneously hypertensive rat. *Gut Microbes*, *13*(1), 1–24. https://doi.org/10.1080/19490976.2020.1854642

Xiong, Y., He, Y., Chen, Z., Wu, T., Xiong, Y., Peng, Y., Yang, X., Liu, Y., Zhou, J., Zhou, H., Zhang, W., Shu, Y., Li, X., & Li, Q. (2023). Lactobacillus induced by irbesartan on spontaneously hypertensive rat contribute to its antihypertensive effect. *Journal of Hypertension*, *42*, 460–470. https://doi.org/10.1097/HJH.0000000000003613

Yang, T., Aquino, V., Lobaton, G. O., Li, H., Colon-Perez, L., Goel, R., Qi, Y., Zubcevic, J., Febo, M., Richards, E. M., Pepine, C. J., & Raizada, M. K. (2019). Sustained captopril-induced reduction in blood pressure is associated with alterations in gut-brain Axis in the spontaneously hypertensive rat. *Journal of the American Heart Association*, *8*(4), e010721. https://doi.org/10.1161/JAHA.118.010721

Yang, T., Mei, X., Tackie-Yarboi, E., Akere, M. T., Kyoung, J., Mell, B., Yeo, J. Y., Cheng, X., Zubcevic, J., Richards, E. M., Pepine, C. J., Raizada, M. K., Schiefer, I. T., & Joe, B. (2022). Identification of a gut commensal that compromises the blood pressure-lowering effect of Ester angiotensin-converting enzyme inhibitors. *Hypertension (Dallas, Tex. : 1979)*, *79*, 1591–1601. https://doi.org/10.1161/HYPERTENSIONAHA.121.18711

Yang, T., Santisteban, M. M., Rodriguez, V., Li, E., Ahmari, N., Carvajal, J. M., Zadeh, M., Gong, M., Qi, Y., Zubcevic, J., Sahay, B., Pepine, C. J., Raizada, M. K., & Mohamadzadeh, M. (2015). Gut dysbiosis is linked to hypertension. *Hypertension (Dallas, Tex. : 1979)*, *65*, 1331–1340. https://doi.org/10.1161/HYPERTENSIONAHA.115.05315

Zarzuelo, M. J., Jiménez, R., Galindo, P., Sánchez, M., Nieto, A., Romero, M., Quintela, A. M., López-Sepúlveda, R., Gómez-Guzmán, M., Bailón, E., Rodríguez-Gómez, I., Zarzuelo, A., Gálvez, J., Tamargo, J., Pérez-Vizcaíno, F., & Duarte, J. (2011). Antihypertensive effects of peroxisome proliferator-activated receptor-β activation in spontaneously hypertensive rats. *Hypertension (Dallas, Tex. : 1979)*, *58*(4), 733–743. https://doi.org/10.1161/HYPERTENSIONAHA.111.174490

Zhernakova, A., Kurilshikov, A., Bonder, M. J., Tigchelaar, E. F., Schirmer, M., Vatanen, T., Mujagic, Z., Vila, A. V., Falony, G., Vieira-Silva, S., Wang, J., Imhann, F., Brandsma, E., Jankipersadsing, S. A., Joossens, M., Cenit, M. C., Deelen, P., Swertz, M. A., LifeLines cohort study, … Fu, J. (2016). Population-based metagenomics analysis reveals markers for gut microbiome composition and diversity. *Science (New York, N.Y.)*, *352*(6285), 565–569. https://doi.org/10.1126/science.aad3369

Zubcevic, J., Richards, E. M., Yang, T., Kim, S., Sumners, C., Pepine, C. J., & Raizada, M. K. (2019). Impaired autonomic nervous system-microbiome circuit in hypertension. *Circulation Research*, *125*(1), 104–116. https://doi.org/10.1161/CIRCRESAHA.119.313965

SUPPORTING INFORMATION

Additional supporting information can be found online in the Supporting Information section at the end of this article.

How to cite this article: González-Correa, C., Moleón, J., Miñano, S., Robles-Vera, I., Toral, M., Barranco, A. M., Martín-Morales, N., O'Valle, F., Guerra-Hernández, E., Sánchez, M., Gómez-Guzmán, M., Jiménez, R., Romero, M., & Duarte, J. (2024). Differing contributions of the gut microbiota to the blood pressure lowering effects induced by first-line antihypertensive drugs. *British Journal of Pharmacology*, 1–25. https://doi.org/10.1111/bph.16410